ResearchGate

See discussions, stats, and author profiles for this publication at: https://www.researchgate.net/publication/347445970

Evolutionary expansion and functional divergence of sugar transporters in Saccharum (S. spontaneum and S. officinarum)

Article *in* The Plant Journal · December 2020

CITATIONS
15

READS
593

9 authors, including:

Qing Zhang
Fujian Agriculture and Forestry University
54 PUBLICATIONS **1,509** CITATIONS

SEE PROFILE

Xiuting Hua
Guangxi University
51 PUBLICATIONS **761** CITATIONS

SEE PROFILE

Yuan Yuan
Guangxi University
11 PUBLICATIONS **547** CITATIONS

SEE PROFILE

Zhengchao Wang
Fujian Normal University
104 PUBLICATIONS **1,520** CITATIONS

SEE PROFILE

All content following this page was uploaded by Jisen Zhang on 18 December 2020.

The user has requested enhancement of the downloaded file.

the plant journal

The Plant Journal (2020) doi: 10.1111/tpj.15076

Evolutionary expansion and functional divergence of sugar transporters in *Saccharum* (*S. spontaneum* and *S. officinarum*)

Qing Zhang[1,†], Xiuting Hua[1,†], Hong Liu[1,†], Yuan Yuan[2], Yan Shi[1], Zhengchao Wang[2], Muqing Zhang[3], Ray Ming[1,4] and Jisen Zhang[1,3,*]

[1]*Center for Genomics and Biotechnology, Haixia Institute of Science and Technology, Fujian Provincial Laboratory of Haixia Applied Plant Systems Biology, College of Life Sciences, Fujian Agriculture and Forestry University, Fuzhou 350002, China,*
[2]*College of Life Sciences, Fujian Normal University, Fuzhou 350117, China,*
[3]*Guangxi key lab for sugarcane biology, Guangxi University, Nanning, Guangxi 530005, China, and*
[4]*Department of Plant Biology, University of Illinois at Urbana-Champaign, Urbana, IL 61801, USA*

Received 19 February 2020; revised 27 October 2020; accepted 4 November 2020.
*For correspondence (e-mail zjisen@fafu.edu.cn).
†These authors contributed equally to this work.

SUMMARY

The *sugar transporter* (*ST*) family is considered to be the most important gene family for sugar accumulation, but limited information about the *ST* family in the important sugar-yielding crop *Saccharum* is available due to its complex genetic background. Here, 105 *ST* genes were identified and clustered into eight subfamilies in *Saccharum spontaneum*. Comparative genomics revealed that tandem duplication events contributed to *ST* gene expansions of two subfamilies, *PLT* and *STP*, in *S. spontaneum*, indicating an early evolutionary step towards high sugar content in *Saccharum*. The analyses of expression patterns were based on four large datasets with a total of 226 RNA sequencing samples from *S. spontaneum* and *Saccharum officinarum*. The results clearly demonstrated 50 *ST* genes had different spatiotemporal expression patterns in leaf tissues, 10 *STs* were specifically expressed in the stem, and 10 *STs* responded to the diurnal rhythm. Heterologous expression experiments in the defective yeast strain EBY.VW4000 indicated STP13, pGlcT2, VGT3, and TMT4 are the STs with most affinity for glucose/fructose and SUT1_T1 has the highest affinity to sucrose. Furthermore, metabolomics analysis suggested *STP7* is a sugar starvation-induced gene and *STP13* has a function in retrieving sugar in senescent tissues. *PLT11*, *PLT11_T1*, *TMT3*, and *TMT4* contributed to breaking the limitations of the storage sink. *SUT1*, *SUT1_T1*, *PLT11*, *TMT4*, *pGlcT2*, and *VGT3* responded for different functions in these two *Saccharum* species. This study demonstrated the evolutionary expansion and functional divergence of the *ST* gene family and will enable the further investigation of the molecular mechanism of sugar metabolism in *Saccharum*.

Keywords: sugar transporter, evolutionary expansion, functional divergence, *Saccharum spontaneum*, *Saccharum officinarum*.

INTRODUCTION

Sugars, including sucrose, monosaccharides, and polyols, are important products of photosynthesis in higher plants, which are not only responsible for plant growth and development, but also serve as important signaling molecules that participate in the regulation of metabolic processes. In plants, the sugars produced by the photosynthetic organs (source) are transported by the phloem over long distances to heterotrophic organs (sink), which receive a constant supply of carbohydrates for their growth and development (Lemoine, 2000). Both loading and unloading of phloem vessels or companion cells mainly depend on sugar transporters (STs) that mediate the transport of monosaccharides (Buttner, 2007), polyols (Noiraud *et al.*, 2001; Juchaux-Cachau *et al.*, 2007), or sucrose (Kühn, 2003; Kühn and Grof, 2010), which are associated with the allocation of sugars in the sink cells. Therefore, further analysis of the evolution and functions of plant STs becomes more and more important in the sugar industry.

At present, the research related to STs has made rapid progress in many species of plants, but research in *Saccharum spontaneum* and *Saccharum officinarum* is very

© 2020 Society for Experimental Biology and John Wiley & Sons Ltd

limited. The *ST* gene family belongs to the major facilitator superfamily (MFS), which is characterized by 12 transmembrane domains (TMDs) (Chang *et al.*, 2004), while the recently identified Sugar Will Eventually be Exported Transporter (SWEET) family of STs belongs to a different superfamily, which is characterized by seven TMDs (Chen *et al.*, 2010; Chen *et al.*, 2012; Xuan *et al.*, 2013). Currently recognized subfamilies of the MFS can be divided into the sucrose transporter family (SUTs) (Riesmeier *et al.*, 1992) and the monosaccharide transporter family (MSTs), while the latter includes the sugar transporter family (STPs) or hexose transporter family (HTs), the plastidic glucose transporter family (pGlcTs), the vacuolar glucose transporter family (VGTs), the tonoplast monosaccharide transporter family (TMTs), the inositol transporter family (INTs/ITRs), the polyol transporter family (PLTs/PMTs), and the sugar facilitator protein family (SFPs) (also known as the early response to dehydration 6-like [ERD6-like] family) (Afoufa-Bastien *et al.*, 2010; Reuscher *et al.*, 2014). Since the cloning of *STP*/*HT*, *SUT*, and *PLT* by Sauer and Tanner (1989) in plants, the *ST* gene families have been identified in various species including Arabidopsis (*Arabidopsis thaliana*) (Buttner, 2007; Sauer, 2007), pear (*Pyrus*) (Li *et al.*, 2015), tomato (*Solanum lycopersicum*) (Reuscher *et al.*, 2014), grape (*Vitis vinifera*) (Afoufa-Bastien *et al.*, 2010), and rice (*Oryza sativa*) (Aoki *et al.*, 2003; Johnson and Thomas, 2007). In each species, the STs were grouped in a SUT family and seven MST families. In addition, phylogenetic evolutionary analysis of plant MSTs has demonstrated that seven MST families are ancient in land plants (Johnson and Thomas, 2007).

Furthermore, the potential functions of some *ST* genes have been investigated in previous studies, but information with respect to their roles in sugarcane (*Saccharum* spp.) is very limited, and further investigations are needed. Previous studies have demonstrated that ZmSUT1 (Carpaneto *et al.*, 2005) and AtSUT4 (Schneider *et al.*, 2012) mediate the active efflux of sucrose at the plasma membrane, and the ERD6-like transporter is likely involved in energy-independent sugar efflux from the vacuole (Poschet *et al.*, 2011; Klemens *et al.*, 2014). However, VGTs and TMTs are implicated in the loading of sugars into the vacuole, as sugar/H^+ antiporters are located in the vacuolar membrane (Wormit *et al.*, 2006; Aluri and Büttner, 2007; Schulz *et al.*, 2011). Heterologous expression of AtSTP1 in *Schizosaccharomyces pombe* and *Xenopusoo cytes* indicated that AtSTP1 is a high-affinity monosaccharide proton symporter capable of transporting various hexose monosaccharides with the exception of fructose (Boorer *et al.*, 1994). AtSTP1 functions in monosaccharide import into guard cells since its transcripts have been detected in guard cells of cotyledons, sepals, rosette leaves, ovaries, and stems (Stadler *et al.*, 2003), while AtSTP2 is found specifically in pollen and likely plays an important role in the uptake of glucose derived from cellulose degradation during the early phase of pollen maturation (Truernit *et al.*, 1999). Recent research demonstrated that AtSTP13 phosphorylation of threonine-485 can enhance monosaccharide uptake activity to compete with bacteria for extra-cellular sugars, which provides a strategy that can be deployed against microbial infections through the regulation of host STs (Yamada *et al.*, 2016). This function is similar to that of a recently evolved STP variant which has also been found in wheat (*Triticum aestivum*) (Moore *et al.*, 2015). Some STs have been characterized in green plants and the pleiotropy of STs was described in many species (Julius *et al.*, 2017). Therefore, analysis of these orthologs in different species might help improve our understanding of their biological functions.

Notably, sugarcane is an economically important bio-energy crop species, which is responsible for approximately 80% of sugar production and 40% of ethanol production worldwide (Zhang *et al.*, 2014). Modern sugarcane cultivars are allopolyploids and interspecific hybrids that are mostly derived from crosses between *S. officinarum* (with high sugar content) and *S. spontaneum* (with high stress tolerance), followed by backcrosses with *S. officinarum*, resulting in about 80% of chromosomes from *S. officinarum* and 10–20% from *S. spontaneum*. Interestingly, *S. officinarum* contains a remarkably high sugar content of up to 21% of juice in the stem (Sreenivasan and Nair, 1991), while less than 6% of sugar contents are stored (Bull and Glasziou, 1963). The sugarcane genome was not available until the end of 2018 (Zhang *et al.*, 2018), and therefore only limited characterization of the *ST* gene family has been reported in sugarcane, with the exception of *SUT* gene family (Zhang *et al.*, 2016). In a previous study, six SUT members were identified based on bacterial artificial chromosomes (BACs), and *SUT1* and *SUT4* were expected to be the main members of the sucrose transporter family as they are expressed abundantly under different conditions (Zhang *et al.*, 2016). In addition, earlier studies based on a survey of the sugarcane expressed sequence tag database demonstrated that *SUT1* expression is higher in mature internodes than in other tissues, which was confirmed by a study in a Hawaiian sugarcane cultivar (Casu *et al.*, 2003; ElSayed *et al.*, 2010). Biochemical analysis of sugarcane SUT1 indicated that it is highly selective, with relatively low affinity for sucrose, and that it is inhibited by sucralose (Rae *et al.*, 2005; Reinders *et al.*, 2006). Therefore, it is important to analyze evolutionary changes and physiological functions of ST in sugarcane (*S. spontaneum* and *S. officinarum*).

In order to reveal the molecular and evolutionary characterization as well as the potential functions of the *ST* gene family in sugarcane, in the present study we characterized the sugarcane *ST* gene family and we performed phylogenetic analysis based on comparative genomic strategies

© 2020 Society for Experimental Biology and John Wiley & Sons Ltd,

with the *S. spontaneum* genome. Furthermore, we also investigated the changes in expression levels of representative *ST* genes, and metabolic levels in two founding *Saccharum* species (*S. spontaneum* and *S. officinarum*), which have differing sugar contents, were examined. The heterologous expression of *ST* genes was performed in defective yeast to assist in predicting their potential functions. The present study assists in revealing the roles of *ST* genes in sugarcane carbohydrate allocation and metabolism and provides gene resources for future genetic improvements in sugarcane breeding.

RESULTS

Identification of *ST* genes

The hidden Markov model-based HMMER profile of the Pfam *Sugar_tr* domain (PF00083) was used as a query for identifying *ST* genes in *S. spontaneum* (Zhang *et al*., 2018). Amino acid sequences that contain the *Sugar_tr* domain were obtained and then used as a query for BLASTP against the published *ST* genes in *A. thaliana* (Buttner, 2007), *O. sativa* (Johnson and Thomas, 2007), and *V. vinifera* (Afoufa-Bastien *et al*., 2010) for further confirmation. We identified 105, 62, 45, 26, 2, and 26 reliable *ST* genes from *S. spontaneum*, *Sorghum bicolor*, *Ananas comosus*, *Amborella trichopoda*, *Chlamydomonas reinhardtii*, and yeast, respectively (Figure 1a), which were then divided into eight subfamilies (one sucrose transporter family and seven monosaccharide transporter families) (Figure 1b).

In *S. spontaneum*, the eight subfamilies are represented by 4–35 members, for example, 4, 4, and 35 members in VGTs, INTs, and STPs, respectively. These *S. spontaneum ST* genes encode proteins with lengths of 202 (SsSFP2_T1, Sspon.007D0001280) to 746 (SsTMT2, Sspon.008C0000240) amino acids, molecular weights ranging from 21.30 (SsSFP2_T1, Sspon.007D0001280) to 79.65 (SsTMT4, Sspon.004A0018790) kDa, 4 to 12 transmembrane domains, and predicted isoelectric points (pI) from pH = 4.78 (SsTMT2, Sspon.008C0000240) to pH = 9.92 (SsSTP30, Sspon.007A0011041) (Tables 1–3 and Table S2). The prediction of subcellular localization by WoLF PSORT revealed that 65.7% (69 out of 105) of *S. spontaneum* STs locate to the plasmalemma (Tables 1–3 and Figure S2).

Phylogenetic analysis of *ST* genes among *S. spontaneum* and other plants

To illustrate the phylogenetic relationship of *ST* gene families in *S. spontaneum*, a total of 429 ST amino acid sequences identified from nine species were used to generate a neighbor-joining (NJ) phylogenetic tree with *ST* genes from *C. reinhardtii* and yeast as the outgroup. According to unique signature motifs or domains from alignments of protein sequences, all these 429 *STs* were classified into eight subfamilies (two large subfamilies and six small families) (Figure 1b). Among these subfamilies, STP and PLT were observed with more gene expansion in monocot species than other subfamilies, while SFP showed more gene expansion in dicot species (Figure 2, Figure S1, and Table 4). Remarkably, *S. spontaneum* had the largest ST families in comparison to these examined plant species, which provided the genetic foundation for high sugar content in *Saccharum*. PLT and STP were found to have more gene members in *S. spontaneum* compared to its closest diploid relative species, indicating that these two subfamilies might have expanded in *S. spontaneum* and that there is a different developmental model for the ST family in monocots and dicots.

To further elucidate the evolutionary relationship of ST subfamilies in *S. spontaneum*, we performed phylogenetic analysis for the subfamilies of *S. spontaneum* and eight other species.

In the STP subfamily, 155 members were divided into six clades, with one of them as the outgroup (Clade 6). Of these six clades, Clades 1, 2, and 3 showed more expansion (two in Clades 1 and 2, four in Clade 3) events, while Clades 4 and 5 were much more conservative in terms of expansion (Figure 2a). Noteworthily, *SsSTP14* (*Sspon.002B0018890*) within Clade 4 was clustered with *A. comosus* and representative dicot species (*A. trichopoda*, *A. thaliana*, and *V. vinifera*), indicating that *SsSTP14* was specifically retained in *S. spontaneum* after the divergence of dicots and monocots; both *SsSTP30* (*Sspon.007A0011041*) and *SsSTP13* (*Sspon.001D0006360*) were phylogenetically distributed with one *A. comosus* STP (*AcoSTP13*) in Clade 5, while *O. sativa* and *S. bicolor* only contained one STP (*OsSTP13* [*Os03g0218400*] and *SbSTP8* [*Sobic.002G073600*], respectively), revealing *Sspon.007A0011041-SsSTP30* were retained from the ρ-whole genome duplication (WGD) before the grass family diverged from its ancestor, with the duplicated genes being lost in *O. sativa* and *S. bicolor*.

In the PLT subfamily, 81 members from eight species were clustered into three clades (Figure 2b). Clade 1 was clustered with the outgroups, and Clades 2 and 3 were phylogenetically distributed together, suggesting Clade 1 was retained from the last common ancestor of PLTs in angiosperm. Clade 2 only contained the PLT members from monocots while Clades 1 and 3 contained gene members from both monocots and dicots. These results indicated that PLTs in Clade 2 were retained from the evolutionary event before the divergence of dicots and monocots. In Clade 1, the phylogenetic relationship showed a one-to-one pattern between *S. bicolor* and *S. spontaneum* for the orthologs in PLTs, indicating the conservation after the split of the two plant species. But in Clades 2 and 3, four sets of tandem gene duplications occurred in *S. spontaneum* after the divergence of *S. bicolor* and *S. spontaneum*, resulting in the gene expansion of PLTs in *S. spontaneum*. For example, *PLT7* (*Sobic.008G111300*) and *PLT2* (*Sobic.005G196700*) in

© 2020 Society for Experimental Biology and John Wiley & Sons Ltd,

(a)

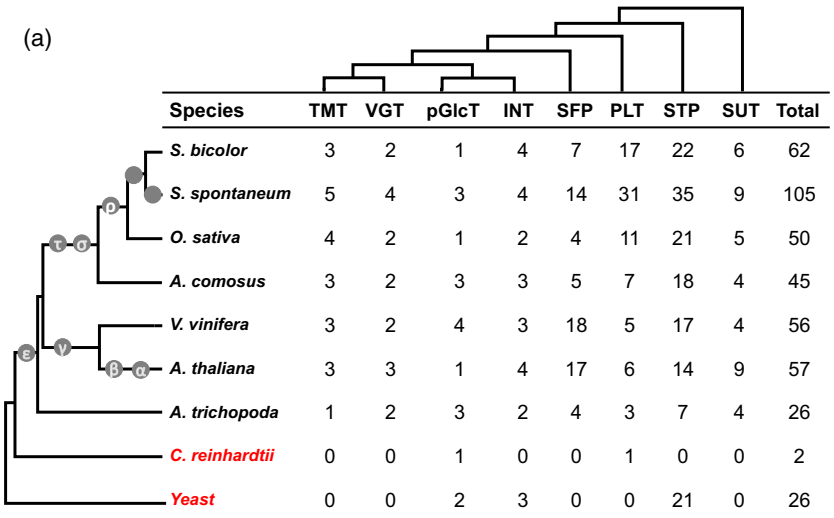

Species	TMT	VGT	pGlcT	INT	SFP	PLT	STP	SUT	Total
S. bicolor	3	2	1	4	7	17	22	6	62
S. spontaneum	5	4	3	4	14	31	35	9	105
O. sativa	4	2	1	2	4	11	21	5	50
A. comosus	3	2	3	3	5	7	18	4	45
V. vinifera	3	2	4	3	18	5	17	4	56
A. thaliana	3	3	1	4	17	6	14	9	57
A. trichopoda	1	2	3	2	4	3	7	4	26
C. reinhardtii	0	0	1	0	0	1	0	0	2
Yeast	0	0	2	3	0	0	21	0	26

(b)

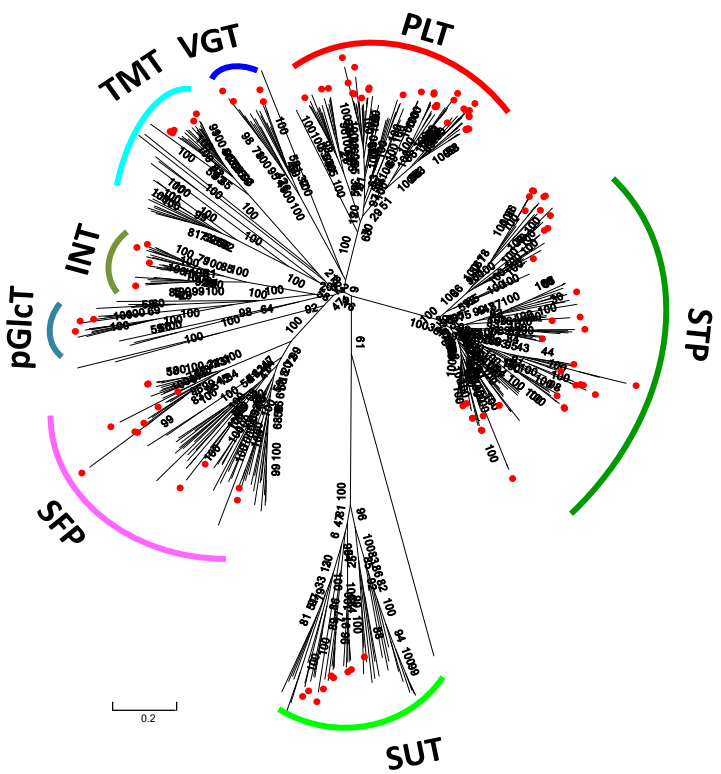

Figure 1. Phylogenetic tree of STs among representative monocotyledons and dicotyledons. (a) The data for angiosperms were used to analyze the hylogenetic relationships of ST families in the present study. The numbers of *ST* genes found in the genome of each species are indicated. (b) The protein sequences were used to build the phylogenetic tree of *STs* among representative monocotyledons and dicotyledons. *ST* genes of *S. spontaneum* are marked with red circles.

S. bicolor were phylogenetically distributed with two and four orthologs in *S. spontaneum* in Clade 2, and two or three copies of *PLT18*, *PLT11*, and *PLT12* were found in *S. spontaneum*.

In the SFP subfamily, the genes were grouped into four clades. Thirteen *SFP* genes in *S. spontaneum* were distributed in three of these four clades (Figure S1), except Clade 1, which only contained the genes from *A. thaliana*. In *S. spontaneum*, SFP numbers were increased in Clade 2, while they were conserved in Clades 3 and 4, with a one-to-one ratio for orthologs between *S. spontaneum* and *S. bicolor*. Furthermore, the results indicated that *SsSFP2*, *SsSFP2_T2*, *SsSFP1_T1*, *SsSFP8_T1*, *SsSFP7*, and *SsSFP8* in Clade 2 originated after the divergence of *S. bicolor* and

© 2020 Society for Experimental Biology and John Wiley & Sons Ltd,

Table 1 Comparison of the details of STP subfamily genes between *Saccharum spontaneum* and *Sorghum bicolor*

	S. spontaneum						*Sorghum bicolor*					
Gene name	Gene ID	Protein	MW (kDa)	TMD	pI	Location*	Ortholog gene ID	Protein	MW (kDa)	TMD	pI	Location
SsSTP1	Sspon.002A0034730	523	57.19	11	9.43	plas	Sobic.002G004900	520	56.89	11	9.25	plas
SsSTP2	Sspon.007C0006820	509	54.48	11	9.58	plas	Sobic.009G152810	244	26.22	4	9.53	plas
SsSTP3	Sspon.003B0019830	509	55.61	12	9.46	vacu	Sobic.003G192200	509	55.73	11	9.39	vacu
SsSTP4	Sspon.002D0004470	531	57.58	11	8.98	plas	Sobic.002G338500	531	57.64	11	9.03	plas
SsSTP5	Sspon.005A0012900	488	53.20	11	9.58	plas	Sobic.006G102800	513	54.04	10	9.18	vacu
SsSTP6	Sspon.001B0021270	518	56.76	11	9.34	vacu	Sobic.001G297600	526	58.02	12	9.29	vacu
SsSTP6_T1	Sspon.001B0039050	524	57.57	12	9.34	plas						
SsSTP6_T2	Sspon.001B0035560	537	58.49	11	9.28	plas						
SsSTP7	Sspon.002D0015220	518	55.73	11	9.30	plas	Sobic.002G201900	518	55.77	11	9.30	plas
SsSTP8	Sspon.002D0025360	512	56.10	9	9.22	plas	Sobic.002G073600	512	56.06	9	9.13	plas
SsSTP9	Sspon.004C0022450	545	59.88	11	9.16	plas	Sobic.004G049300	521	57.24	11	8.91	plas
SsSTP10	Sspon.001A0027320	531	56.14	11	8.80	plas	Sobic.001G190200	533	56.72	11	8.90	plas
SsSTP10_T1	Sspon.001A0027340	527	55.72	11	8.80	vacu						
SsSTP11	Sspon.006A0022080	467	49.83	11	9.74	plas	Sobic.005G171200	524	56.06	12	9.40	vacu
SsSTP11_T1	Sspon.006A0022081	493	52.38	12	9.33	vacu						
SsSTP11_T2	Sspon.006A0022100	451	47.91	11	9.02	vacu						
SsSTP11_T3	Sspon.006A0022101	457	48.53	9	9.30	vacu						
SsSTP12	Sspon.006C0013410	514	55.64	11	8.10	plas	Sobic.007G061800	521	56.26	11	8.06	plas
SsSTP13	Sspon.001D0006360	517	56.94	11	8.93	plas	Sobic.001G454100	517	56.98	12	9.04	plas
SsSTP14	Sspon.002B0018890	518	56.66	10	9.14	plas	N/A	N/A	N/A	N/A	N/A	N/A
SsSTP16	Sspon.008D0020290	508	53.65	10	9.63	vacu	Sobic.010G030600	521	54.58	12	9.81	vacu
SsSTP17	Sspon.007C0006791	538	56.38	9	9.45	plas	Sobic.009G152800	480	51.53	10	8.73	plas
SsSTP18	Sspon.005A0012842	463	50.20	11	9.47	plas	Sobic.006G101900	542	57.73	11	9.77	plas
SsSTP19	Sspon.004A0012530	466	51.15	10	9.43	plas	Sobic.004G188701	488	53.12	7	8.86	vacu
SsSTP20	Sspon.005A0012960	499	53.26	10	9.63	vacu	Sobic.006G102500	510	54.31	11	9.51	vacu
SsSTP20_T1	Sspon.005A0012880	491	52.42	10	9.69	vacu						
SsSTP22	Sspon.005C0016850	490	53.27	11	9.14	vacu	Sobic.006G003600	516	56.39	11	9.32	vacu
SsSTP22_T1	Sspon.005C0016840	490	53.27	11	9.14	vacu						
SsSTP25	Sspon.005A0012970	463	50.20	11	9.47	plas	Sobic.006G102400	521	55.69	10	9.25	plas
SsSTP25_T1	Sspon.005A0012841	512	54.11	10	9.58	vacu						
SsSTP28	Sspon.005A0012930	484	52.97	11	9.49	vacu	Sobic.006G102300	511	55.33	11	9.40	vacu
SsSTP28_T1	Sspon.005A0012940	438	47.77	10	9.76	plas						
SsSTP29	Sspon.004D0003010	526	56.02	11	9.20	plas	Sobic.004G332700	523	55.63	11	9.12	plas
SsSTP29_T1	Sspon.004D0002960	526	56.02	11	9.20	plas						
SsSTP30	Sspon.007A0011041	364	41.14	7	9.92	plas	N/A	N/A	N/A	N/A	N/A	N/A

*plas, plasmalemma; vacu, vacuole; MW, molecular weight; TMD, transmembrane domain; pI, isoelectric point.

© 2020 Society for Experimental Biology and John Wiley & Sons Ltd,

Table 2 Comparison of the details of PLT subfamily genes between *Saccharum spontaneum* and *Sorghum bicolor*

	S. spontaneum						*Sorghum bicolor*					
Gene name	Gene ID	Protein	MW (kDa)	TMD	pI	Location*	Ortholog gene ID	Protein	MW (kDa)	TMD	pI	Location
SsPLT1	Sspon.006D0022390	483	50.57	9	8.97	vacu	Sobic.005G195900	481	50.34	9	8.96	vacu
SsPLT2	Sspon.006C0021080	479	50.13	12	8.94	vacu	Sobic.005G196700	485	50.94	12	8.36	vacu
SsPLT2_T1	Sspon.006C0021090	478	50.00	12	8.80	vacu						
SsPLT2_T2	Sspon.006C0021120	499	52.45	12	8.41	vacu						
SsPLT2_T3	Sspon.006C0020960	478	49.99	12	8.74	vacu						
SsPLT3	Sspon.002A0037081	530	55.47	11	9.39	plas	Sobic.008G111100	616	63.69	12	9.47	plas
SsPLT4	Sspon.005A0008730	533	57.48	9	5.55	plas	Sobic.006G156600	726	78.98	11	8.73	plas
SsPLT5	Sspon.006B0022900	434	45.18	10	8.73	vacu	Sobic.005G196300	490	50.84	10	5.85	vacu
SsPLT6	Sspon.005D0018230	515	54.46	12	9.61	vacu	Sobic.009G157800	530	55.72	12	9.58	vacu
SsPLT7	Sspon.002A0037110	480	50.14	12	9.13	plas	Sobic.008G111300	491	51.50	10	8.99	plas
SsPLT7_T1	Sspon.002A0037100	487	51.25	10	8.20	plas						
SsPLT8	Sspon.006D0022420	485	50.80	10	8.78	plas	N/A	N/A	N/A	N/A	N/A	N/A
SsPLT9	Sspon.005A0001151	541	57.24	10	7.53	vacu	Sobic.006G268790	430	44.90	7	6.96	plas
SsPLT10	Sspon.005D0000761	502	52.00	10	7.76	vacu	Sobic.006G268800	536	55.56	11	6.42	plas
SsPLT11	Sspon.001B0005390	521	55.85	11	8.85	plas	Sobic.001G469600	524	56.12	11	8.84	plas
SsPLT11_T1	Sspon.001B0005380	521	55.85	11	8.85	plas						
SsPLT12	Sspon.001D0005580	525	55.90	10	8.60	plas	Sobic.009G084400	524	55.40	10	6.03	plas
SsPLT12_T1	Sspon.001D0005841	522	55.61	12	7.72	plas						
SsPLT12_T2	Sspon.001D0005870	515	55.06	12	8.29	plas						
SsPLT13	Sspon.001A0015850	536	57.01	10	8.90	plas	Sobic.001G323600	535	56.94	10	8.55	plas
SsPLT13_T1	Sspon.001A0008970	538	57.22	10	8.90	plas						
SsPLT14	Sspon.002C0007270	328	34.60	6	5.51	vacu	Sobic.002G354100	505	54.03	11	8.94	plas
SsPLT15	Sspon.002A0026520	589	61.89	10	8.99	plas	Sobic.005G196100	507	52.63	11	9.11	plas
SsPLT15_T1	Sspon.006A0023850	485	51.51	10	9.81	plas						
SsPLT16	Sspon.006A0023830	484	50.55	9	8.77	vacu	Sobic.005G196000	491	51.29	10	8.90	vacu
SsPLT16_T1	Sspon.006A0023831	495	51.35	11	8.46	plas						
SsPLT17	Sspon.002C0007250	511	54.44	12	8.92	vacu	Sobic.002G353900	510	54.22	12	9.16	vacu
SsPLT17_T1	Sspon.002C0007280	504	53.97	11	8.80	plas						
SsPLT18	Sspon.002C0007330	480	50.72	10	9.05	vacu	Sobic.002G354000	510	53.91	12	8.78	vacu
SsPLT18_T1	Sspon.002C0007290	509	53.81	11	8.73	vacu						
SsPLT18_T2	Sspon.002C0007310	432	46.16	8	9.40	plas						

*plas, plasmalemma; vacu, vacuole; MW, molecular weight; TMD, transmembrane domain; pI, isoelectric point.

S. spontaneum, given that their closest orthologs in *S. bicolor* were phylogenetically distributed as outgroups.

In the SUT subfamily, 41 *SUTs* from seven species were divided into five groups (*SUT1* to *SUT5*) (Figure S2), which were consistent with previous studies (Kühn and Grof, 2010; Deol *et al.*, 2013; Milne *et al.*, 2013). Among these five groups, the genes in the *SUT1* group were found only in dicotyledons, while the genes in the *SUT3* and *SUT5* groups were found only in monocotyledons. The other two groups, *SUT2* and *SUT4*, were found in both dicotyledons and monocotyledons, and classified into two distinct subclades. In *S. spontaneum*, three copies of tandem duplicated *SsSUT2* were found in the *SUT2* group and two copies of tandem duplicated *SsSUT3* were distributed in the *SUT3* group, while these two groups only contained a single *SUT* from *S. bicolor*. These results indicated that the tandem duplications of *SsSUT1* and *SsSUT2* occurred after the split of *S. spontaneum* and *S. bicolor*.

The four ST subfamilies VGT, TMT, pGlcT, and INT were phylogenetically analyzed for seven plant species, and two sets of tandem duplicated genes were found, (i) *SsVGT1* and *SsVGT2* and (ii) *SsVGT3* and *SsVGT3_T1*, that were clustered closely with their *S. bicolor* orthologs (Figure 2c). Similarly, *SsTMT1* and *SsTMT1_T1* tandem couple with *SsTMT2*, which clusters with the orthologs from *S. bicolor*. *SspGlcT2* was clustered with *SbpGlcT2* and *OspGlcT2*, which conforms with their corresponding species evolution, while *SspGlcT1* and *SspGlcT1_T1* tandem cluster with *AcpGlcT1*, indicating *pGlcT1* may be lost from the grass family except in *S. spontaneum*. In addition, *SsINT1*, *2*, *3*, and *4* were clustered with single-copy orthologs from *S. bicolor*, indicating the genes of the INT subfamily in *S. spontaneum* were conserved during evolution. These results provided additional evidence that tandem duplications contributed to the gene expansion of STs in *S. spontaneum*.

© 2020 Society for Experimental Biology and John Wiley & Sons Ltd,

Table 3 Comparison of the details of SFP, pGlcT, TMT, INT, and VGT subfamily genes between *Saccharum spontaneum* and *Sorghum bicolor*

	S. spontaneum						*Sorghum bicolor*					
Gene name	Gene ID	Protein	MW (kDa)	TMD	pI	Location*	Ortholog gene ID	Protein	MW (kDa)	TMD	pI	Location
SsSFP1	Sspon.007D0002170	324	35.24	9	5.23	vacu	Sobic.009G235600	499	53.65	12	8.91	plas
SsSFP1_T1	Sspon.007D00021701	666	71.17	10	9.31	plas	N/A	N/A	N/A	N/A	N/A	N/A
SsSFP2	Sspon.007D0001270	459	49.19	11	9.53	plas	Sobic.009G243800	507	54.12	12	9.23	plas
SsSFP2_T1	Sspon.007D0001280	202	21.30	4	6.23	plas						
SsSFP2_T2	Sspon.007D0001301	486	52.00	11	9.20	plas						
SsSFP4	Sspon.001A0012461	527	57.55	11	9.46	plas	Sobic.001G362500	505	53.92	10	6.47	vacu
SsSFP4_T1	Sspon.001A0012462	526	56.38	12	5.65	vacu						
SsSFP5	Sspon.003A0022130	394	41.60	8	8.40	vacu	Sobic.003G111000	488	51.69	12	8.33	plas
SsSFP6	Sspon.003B0027210	427	45.36	9	5.85	vacu	Sobic.003G110800	486	51.78	12	6.24	plas
SsSFP7	Sspon.007D0002100	392	42.90	6	6.43	plas	Sobic.009G235700	506	53.70	12	7.49	plas
SsSFP8	Sspon.007D0001962	559	60.36	9	9.07	plas	Sobic.009G235900	501	54.03	12	7.68	plas
SsSFP8_T1	Sspon.007D0001963	383	40.61	8	8.83	plas						
SsSFP8_T2	Sspon.007D0001964	433	46.57	10	5.26	plas						
SspGlcT1	Sspon.002B0016870	553	58.65	9	6.21	plas	N/A	N/A	N/A	N/A	N/A	N/A
SspGlcT1_T1	Sspon.002B0016812	441	47.42	9	5.36	plas						
SspGlcT2	Sspon.004C0017071	484	52.22	10	8.64	E.R.	Sobic.004G124500	490	52.48	10	8.64	plas
SsTMT1	Sspon.004D0000100	692	72.55	10	5.10	plas	Sobic.004G358100	498	52.30	5	9.39	plas
SsTMT1_T1	Sspon.004D0000240	679	71.14	10	5.05	plas						
SsTMT2	Sspon.008C0000240	746	79.00	11	4.78	plas	Sobic.010G276100	767	81.65	11	4.76	plas
SsTMT3	Sspon.001A0016560	732	78.11	10	4.88	vacu	Sobic.001G312900	740	78.91	10	4.91	vacu
SsTMT4	Sspon.004A0018790	745	79.65	11	5.16	plas	Sobic.004G099300	746	79.65	11	5.16	plas
SsINT1	Sspon.005C0003130	506	53.79	12	5.40	plas	Sobic.006G130800	506	53.93	12	5.67	plas
SsINT2	Sspon.002B0029970	585	62.53	12	8.68	plas	Sobic.002G035200	586	62.55	12	7.96	plas
SsINT3	Sspon.005B0007800	591	64.47	12	8.98	plas	Sobic.006G143900	586	63.18	12	8.52	plas
SsINT4	Sspon.002C0025371	573	61.13	12	8.68	vacu	Sobic.002G121800	574	61.31	12	8.19	vacu
SsVGT1	Sspon.001A0010990	426	46.21	8	6.31	plas	N/A	N/A	N/A	N/A	N/A	N/A
SsVGT2	Sspon.001A0011020	390	42.57	8	7.54	plas	Sobic.001G282600	511	54.81	11	5.29	plas
SsVGT3	Sspon.001A0040123	586	62.43	10	9.83	chlo	Sobic.001G032200	565	59.24	11	9.52	chlo
SsVGT3_T1	Sspon.001A0040181	594	63.38	10	9.76	chlo						

*plas, plasmalemma; vacu, vacuole; MW, molecular weight; TMD, transmembrane domain; pI, isoelectric point.

© 2020 Society for Experimental Biology and John Wiley & Sons Ltd,

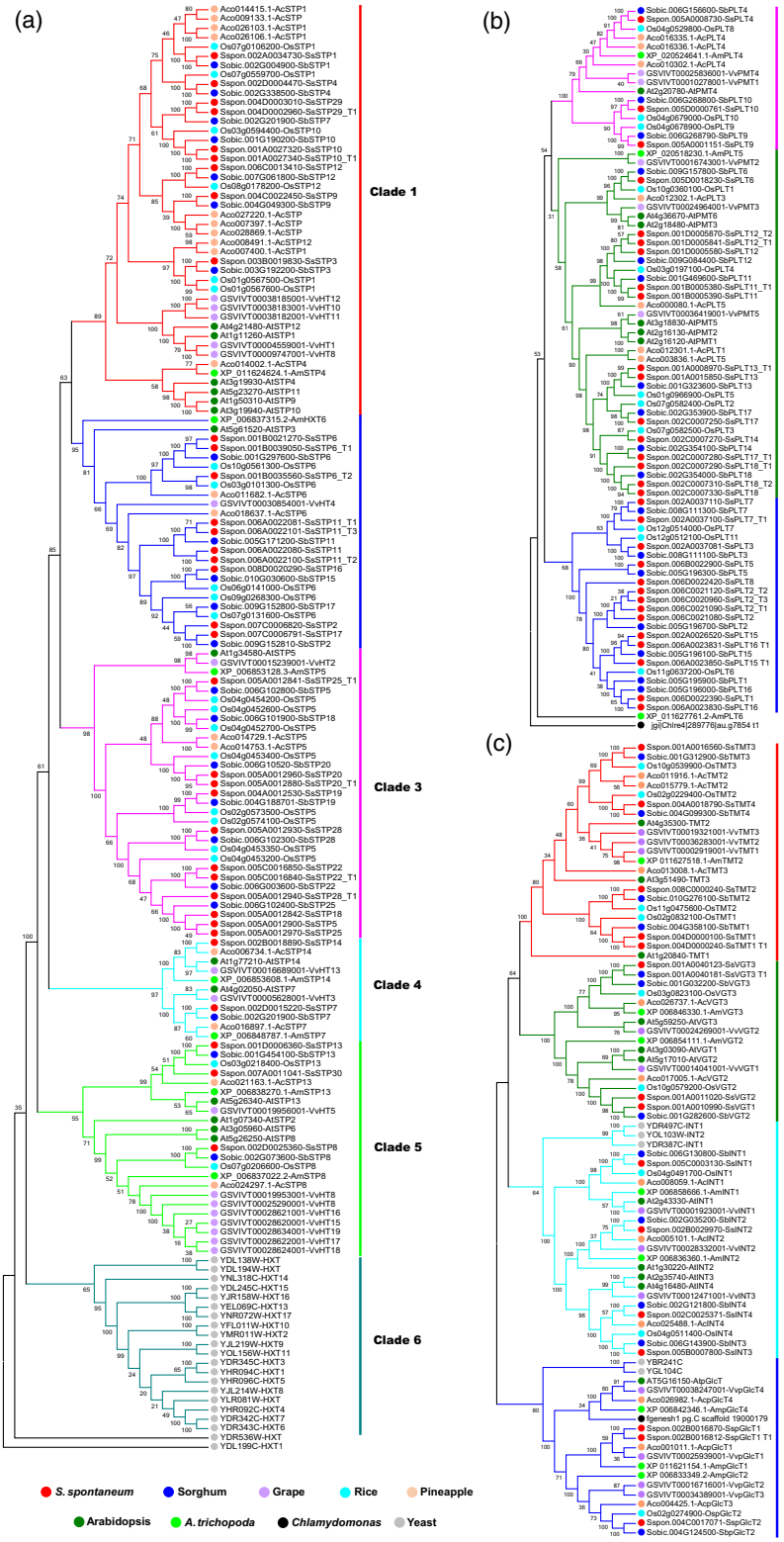

Figure 2. Phylogenetic tree of ST subfamilies among representative monocotyledons and dicotyledons. All phylogenetic trees were built with the neighbor-joining algorithm using protein sequences. (a) The phylogenetic tree of the STP subfamily. (b) The phylogenetic tree of the PLT subfamily. (c) The phylogenetic tree of the VGT, TMT, pGlcT, and INT subfamilies. *ST* genes of *S. spontaneum* in the phylogenetic trees are marked with red, and the remaining STs of other species are marked with different colors as labeled at the bottom.

© 2020 Society for Experimental Biology and John Wiley & Sons Ltd,

Table 4 Comparison of the ST genes in *S. spontaneum* (Ss), *S. bicolor* (Sb), *A. thaliana* (At), and *O. sativa* (Os)

	Number of genes								
Subfamily	Ss	Tandem duplications	Segmental duplications	Sb	Tandem duplications	At	Tandem duplications	Os	Tandem duplications
SFP	14	10	0	7	5	17	10	4	2
pGlcT	3	2	1	1	0	1	0	1	0
TMT	5	2	0	4	0	3	0	4	0
INT	4	0	0	4	0	4	0	2	0
VGT	4	2	0	2	0	3	0	2	0
PLT	31	22	2	17	11	6	2	11	4
STP	35	19	6	22	9	14	2	21	7
SUT	9	5	0	6	0	9	2	5	0
Total	105	62	9	63	25	57	16	50	13

Gene structure and conserved motifs of *S. spontaneum* STs

In order to obtain additional information on the conservation of *S. spontaneum ST* genes, their structures were analyzed with the Gene Structure Display Server (GSDS) online suite and schematically illustrated based on their evolutionary relationships (Figure S3). The number of exons and introns in *S. spontaneum ST* genes ranged from 1 to 20 and from 0 to 19, respectively. Most of the *S. spontaneum* genes in the PLT (93.5%) and STP (82.9%) subfamilies contained two to four exons, indicating that these two gene families were conserved during plant evolution. The gene structure of some subfamilies (VGT, TMT, INT, SFP, and SUT) had a greater diversification with several exon/intron variations. For example, in the SFP subfamily, *Sspon.007D0002100-SsSFP7* and *Sspon.007D0002020-SsSFP9* contained six and 10 exons, respectively, while the remaining members possessed more than 12 exons. In contrast, all *S. spontaneum* genes within the pGlcT subfamily contained 12 or 13 exons, indicating these *S. spontaneum* pGlcT genes share a highly conserved structure.

Additionally, the putative amino acid sequences of *S. spontaneum ST* genes were further analyzed for conserved motifs using MEME suite 4.11.1. A total of 15 conserved motifs were identified in the collective putative ST proteins and designated as Motifs 1–15 based on the E-value of each motif (Figure S3). The most common motif at the N-terminal is Motif 6, which was found in 98 out of 105 (93.3%) *S. spontaneum* STs. Motif 2 was found at the C-terminus in 89 out of 105 (84.8%) *S. spontaneum* STs. No subfamily-specific motif was found in eight subfamilies of *S. spontaneum*, suggesting these gene subfamilies might originate from the same ancestor. Furthermore, 89 out of 96 (92.7%) monosaccharide transporter genes had >12 motifs, while all SUTs possessed <6 motifs, which might be due to their functional differences between the monosaccharide transporter family (which transports monosaccharides) and the SUT family (which transports sucrose) in *S. spontaneum*.

Interestingly, the type and number of conserved motifs were highly similar within each monosaccharide transporter family, indicating functional similarities of these genes within the same family. Some subfamilies shared a similar motif and motif order. For example, the motif order of 3, 6, 9, 14, 5, 10, 4, and 3 was detected in the majority of PLT and STP subfamilies, and the motif orientation 6, 9, 5, and 10 was found in all monosaccharide transporter families, indicating that they shared a close phylogenetic relationship. In addition, some motifs were missing in certain families; for example, the STP subfamily lacked Motif 7; the PLT, VGT, TMT, INT, SFP, and SUT subfamilies lacked Motif 11; and the VGT, TMT, INT, SFP, and SUT subfamilies lacked Motif 15. These results further supported the functional divergence among these ST subfamilies.

Chromosomal localization, duplication events, and collinearity of *S. spontaneum* STs

The distribution of *ST* genes on the *S. spontaneum* chromosome was investigated in this study. Of 105 *S. spontaneum ST* genes, 100 (95.2%) were mapped onto six chromosomes, excluding chromosomes SsChr3 and SsChr8, which represents an unbalanced distribution (Figure 3a,b). Substantial clustering of *S. spontaneum ST* genes was obvious on several chromosomes, especially on those with high densities of ST genes. For example, *SsSTP28*, *SsSTP28_T1*, *SsSTP5*, and *SsSTP18* were clustered and localized on a 92.8-kb segment on SsChr5. In addition, all subfamilies were found to have a differential distribution in the whole genome, such as 10 (25.6%) *STPs* and 11 (35.5%) *PLTs* located on SsChr5 and SsChr2, respectively, while no STs were located on SsChr3 except for three *SsSFPs* (Figure 3c,d).

During the evolution of a gene family, tandem duplication plays an important role in gene family expansion. Therefore, in order to clarify the potential tandem duplication of *S. spontaneum ST*, the collinearity of the *S. spontaneum ST* gene family was identified with BLASTP and Multiple Collinearity Scan (MCScanX). Finally, 62 tandem

© 2020 Society for Experimental Biology and John Wiley & Sons Ltd,

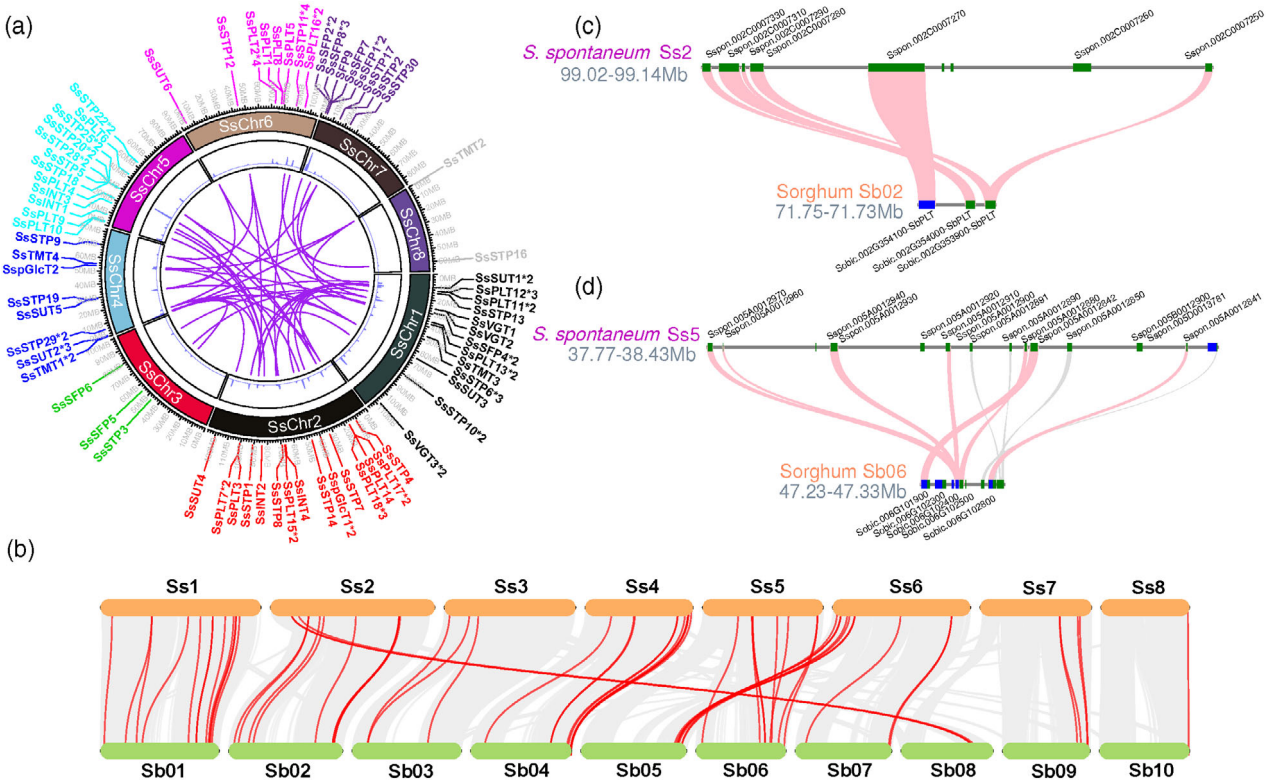

Figure 3. Genome distribution and gene duplication of the *ST* gene family in *S. spontaneum*. (a) The scale on the circle is in Megabases. The numbers of each chromosome are shown inside the circle with different colors. The density of *ST* genes distributed on the chromosome is represented in grayscale. The WGD or segmental duplication genes are connected with a purple line. In addition, after each gene ID, the star annotation indicates the number of copies. For example, *2, *3, and *4 indicate tandem duplication with two, three, and four copies, respectively. (b) Microcollinearity and tandem duplication of PLTs between chromosome 2 of *S. spontaneum* and *S. bicolor*. The genes are represented by green and blue boxes, and the gene ID is shown near the boxes. In addition, the collinear gene pairs are represented by gray lines, and the collinear STP or PLT gene pairs are highlighted by pink lines. (c) Gray lines in the background indicate the collinear blocks within the *S. spontaneum* and *S. bicolor* genomes, while the red lines highlight the syntenic *ST* gene pairs. (d) Microcollinearity and tandem duplication of STPs between chromosome 5 of *S. spontaneum* and chromosome 6 of *S. bicolor*.

duplicated *ST* genes were identified in *S. spontaneum*, which showed that more tandem duplications occurred in *S. spontaneum* compared with *S. bicolor* (25), *A. thaliana* (16), and *O. sativa* (13) (Table 4). All the above tandem duplicated *ST* gene pairs had non-synonymous/synonymous substitution (Ka/Ks) ratios values of less than 1, except for *SsSFP2-SsSFP2_T1*, implying they evolved under the effects of purifying selection (Table S3).

To further investigate possible evolutionary mechanisms of the *S. spontaneum ST* gene family, we also constructed a comparative syntenic map of *S. spontaneum* associated with *S. bicolor*, which is the closest relative with sequenced genome in the grass family. Finally, 61 orthologous pairs were identified between *S. spontaneum* and *S. bicolor* (Figure 3b). Interestingly, the members of PLT and STP subfamilies were assigned to 99.02–99.14 Mbp of Ss2 and 37.77–38.43 Mbp of Ss5, which included all tandem duplication blocks with high collinearity in *S. bicolor* assigned to 71.73–71.75 Mbp of Sb02 and 47.23–47.33 Mbp of Sb06, respectively (Figure 3c,d).

Analysis of expression of *ST* genes during different developmental stages in *S. spontaneum* and *S. officinarum*

To investigate the temporal and spatial expression patterns of *ST* genes in two *Saccharum* species with different sugar content (higher sugar content in *S. officinarum* and lower in *S. spontaneum*), we further analyzed their *ST* transcript abundance (Transcripts Per Million [TPM], normalized data) using the transcriptome data from different development stages, which included two tissues (internode and leaf) from the seedling stage, five tissues (including (i) internodes 3, 6, and 9 for *S. spontaneum* and 3, 9, and 15 for *S. officinarum* and (ii) leaf roll and leaf in both) of the pre-matured and matured stages, 15 leaf segments from a developmental gradient leaf, and the leaves during the diurnal cycle, in addition to parenchymal and sclerenchyma cells of matured internodes in *S. officinarum*. The expression levels of two *ST* genes in five tissues ((i) internodes 3, 9, and 15, leaves, and leaf roll in LA-Purple

© 2020 Society for Experimental Biology and John Wiley & Sons Ltd,

and (ii) internodes 3, 6, and 9, leaves, and leaf roll in SES208) of two *Saccharum* species were validated by quantitative real-time PCR (qRT-PCR) (Figure S4).

The genes with TPM < 15 in each sample of both species within the same dataset are not shown in the heatmap (Figure 4). During different development stages, some genes from both *Saccharum* species showed high expression in specific tissues (Figure 4a,d). For example, *VGT3* and *STP7* were highly expressed in the leaves in three developmental stages and in the leaf roll of the pre-matured and matured stages in both *Saccharum* species, while *TMT3* was highly expressed in internodes, suggesting that *VGT3* and *STP7* may play an important role in the sugar loading of source leaves. Some genes in specific tissues showed higher expression in *S. spontaneum* than in *S. officinarum*; for example, *pGlcT2* showed higher expression in the tested internodes during the pre-matured and matured stages in *S. spontaneum* than in *S. officinarum*, while *SUT1*, *SUT1_T1*, and *TMT4* were highly expressed only in internodes 6 and 9 during the matured and pre-matured stages in *S. spontaneum*, in contrast to internodes 9 and 15 of *S. officinarum* at the same stage. Interestingly, some genes showed a reverse situation, in which expression was higher in specific tissues of *S. officinarum* than in *S. spontaneum*. For example, *PLT11*, *PLT11_T1*, and *STP7* were highly expressed in leaf at the pre-matured stage in *S. officinarum* compared to *S. spontaneum*, while *STP4* was highly expressed in the leaf during the matured and pre-matured stages of *S. spontaneum* compared to *S. officinarum*. In addition, *TMT3*, *TMT4*, *PLT11*, *PLT11_T1*, and *SUT4* were highly expressed in both parenchyma and sclerenchyma cells at the matured stage of *S. officinarum*, while *SUT1* and *SUT1_T1* were highly expressed only in sclerenchyma cells and *SFP4_T1* only in parenchymal cells. These results indicated these STs may play an important role in sclerenchyma and parenchymal cells of *S. officinarum*.

Analysis of *ST* expression during leaf segmental development in *S. spontaneum* and *S. officinarum*

In order to understand the contributions of STs to leaf development and photosynthesis, we divided the leaves of seedlings from *S. spontaneum* and *S. officinarum* into 15 segments from base to tip. We named these segments S1–15 and further divided them into the basal zone (S1–3), the transitional zone (S4–6), the maturing zone (S7–10), and the matured zone (S11–15). The results showed 72 (68.5%) of 105 *STs* from *S. spontaneum* and *S. officinarum* had low expression levels (TPM < 15) throughout all these leaf segments; these data are not shown in Figure 4(b,e). Of the remaining 33 *STs*, some were expressed in a similar pattern in the tested leaf segments of *S. spontaneum* and *S. officinarum*; for example, *SUT1* and *SUT1_T1* had high expression levels in the maturing and matured zones of both species, while *STP4* had high expression levels in the whole leaf segments and much higher expression levels in the maturing and matured zones. Some *STs* exhibited higher expression levels in *S. officinarum* than in *S. spontaneum*. For example, *VGT3*, *PLT17*, and *STP13* were highly expressed in the matured zone (S11–15), *STP6_T2* was highly expressed in the transitional zone (S4–6), and *PLT11* and *PLT11*_T1 were highly expressed in the maturing zone (S7–10) of *S. officinarum*, while they were lowly expressed in the same segments of *S. spontaneum*. These results indicated that *ST* genes may play an important role in sugar loading in the source leaf.

Given the abundance of tandem duplicated *STs* in the *S. spontaneum* genome, we also statistically analyzed the changes in expression of 62 (26 pairs) tandemly duplicated *STs* (Tables 1–4) to further understand the difference in expression within tandemly duplicated STs pairs. The results indicated that 53.8% (14 pairs) of 26 pairs of the tandemly duplicated *STs* had at least one member expressed in the developmental gradient of the leaves (Figure 4b). Among these, with the exception of *PLT11* and *PLT11_T1*, the remaining 13 pairs had differing expression levels, indicating divergence of gene functions occurred in more than 50% of tandem duplicated *STs* of *S. spontaneum*.

Changes in *ST* expression during the day-night rhythm in matured leaves of *S. spontaneum* and *S. officinarum*

To elucidate the expression patterns and functional roles of *STs* during the day-night rhythm in *S. spontaneum* and *S. officinarum*, we collected matured-stage leaf samples with three replicates from 06:00 am to 06:00+ am every 2 h during cycle 1 and every 4 h during cycle 2, which acted as a replicate, and these samples were used for RNA sequencing (RNA-seq) analysis to evaluate the relative abundance of each of the *STs*. The results identified 72 (68.5%) out of 105 *STs* with low expression (TPM < 15) at all tested time points in both species; these are not included in Figure 4(c, f). The remaining 33 *STs*, for example, *SUT1*, *SUT1_T1*, and *VGT3*, showed high expression during the whole cycle in both species, but the former two genes showed a lack of stable expression at specific time points. For example, *SUT1* and *SUT1_T1* expression in *S. spontaneum* increased from 18:00 to 02:00, while in *S. officinarum*, expression levels increased from 06:00 to 10:00. In contrast, some *STs* were only highly expressed at specific time points; for example, genes such as *VGT2*, *PLT12*, *PLT12_T1*, *PLT17*, *STP4*, and *STP7* were highly expressed at 10:00 in the leaves of *S. officinarum*. Furthermore, *TMT4* was highly expressed in *S. spontaneum* in the time period 12:00 to 18:00, while in *S. officinarum*, *TMT4* was highly expressed between 12:00 and 06:00. In addition, some genes were highly expressed specifically during the cycle of *S. spontaneum*, such as *TMT3*, which showed high

© 2020 Society for Experimental Biology and John Wiley & Sons Ltd,

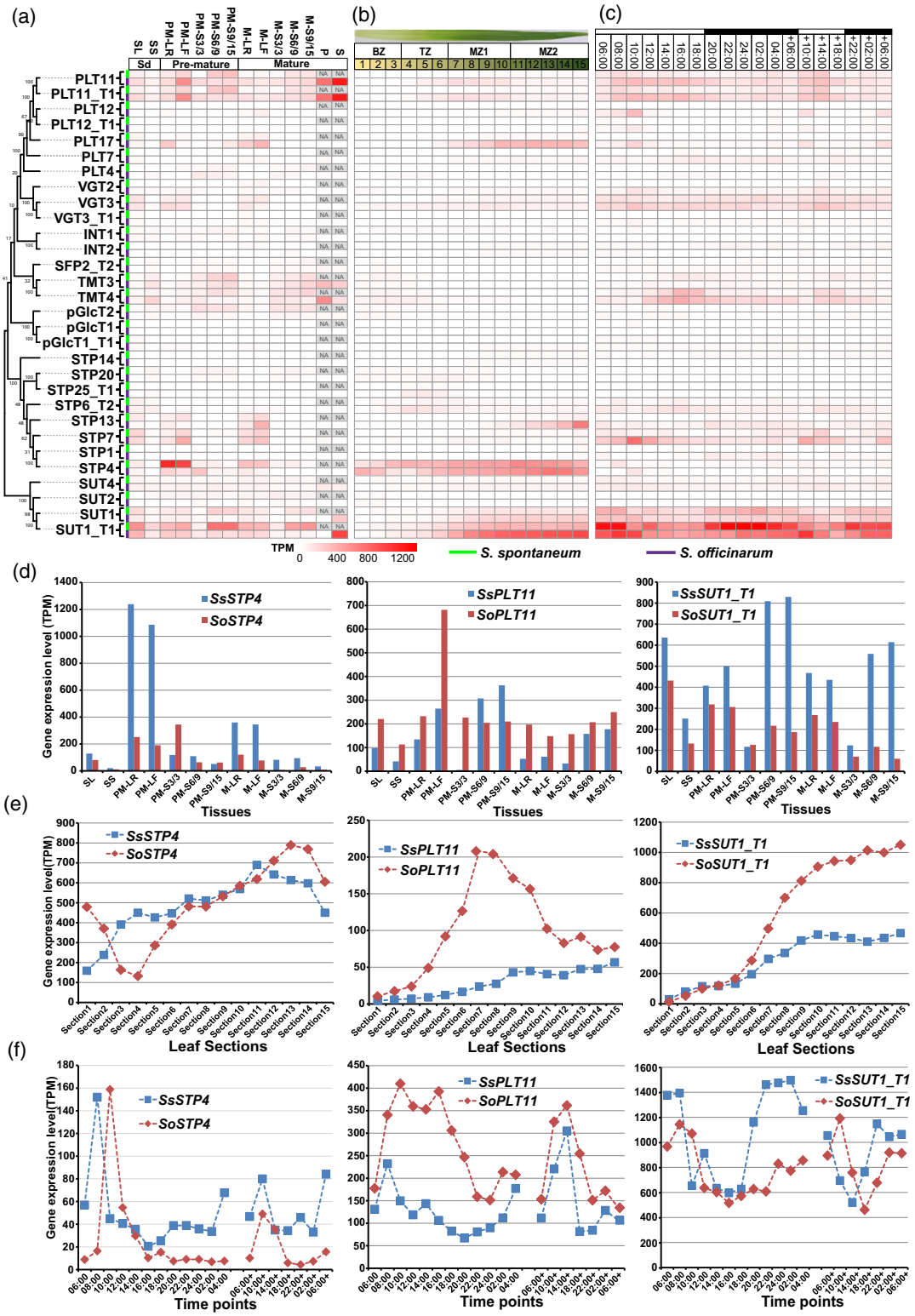

Figure 4. The expression patterns of STs during the three sugar accumulation stages (seedling, pre-matured, and matured stages), leaf gradients and day-night rhythms in *S. spontaneum* and *S. officinarum*. (a,d) The expression patterns of STs based on the RNA-seq data of different tissues during different stages of these two *Saccharum* species and in the parenchyma and sclerenchyma cells of *S. officinarum*. (b,e) The expression patterns of STs based on the RNA-seq data across the leaf gradients of these two *Saccharum* species. (c,f) The expression patterns of STs based on the RNA-seq data at different time periods in these two *Saccharum* species.

© 2020 Society for Experimental Biology and John Wiley & Sons Ltd,

expression only in the matured leaves of *S. spontaneum* within the time frame of 16:00 to 20:00.

Characteristics of sugar metabolism in *S. spontaneum* and *S. officinarum*

In order to profile the primary sugar metabolic changes in stems (including the upper, middle, and bottom parts) and leaves (including the leaf roll and leaf) of matured *S. spontaneum* and *S. officinarum*, we performed a soluble sugar analysis to detect three kinds of sugar (sucrose, fructose, and glucose) by biochemical methods. The results showed that these three sugars exhibited a significant difference in matured leaves and matured stems of *S. spontaneum* and *S. officinarum* (Figure 5a).

Saccharum officinarum had higher concentrations of fructose in matured leaves and matured stems, with the greatest amounts at the bottom of stems, whereas *S. spontaneum* had lower concentrations of fructose in the corresponding tissues (Figure 5a). In contrast, the sucrose concentration was much higher in *S. officinarum* and was similar in the lower matured leaves, and *S. officinarum* was found to contain 600–1000 mg g^{-1} sucrose, which is significantly higher than the sucrose content of *S. spontaneum*, with 22–28 mg g^{-1} in the matured stem. The sucrose concentration was found to increase down the stem, with the highest concentrations at the bottom of the matured stem in *S. officinarum*, whereas in *S. spontaneum* the sucrose concentration was lower and equally distributed throughout the stem (Figure 5a). In addition, the glucose concentration was similar in both *S. spontaneum* and *S. officinarum*, showing an increasing trend from the top towards the bottom of the stem and relatively low levels in leaves, indicating glucose as a basal metabolite was maintained at similar metabolic levels in the mature stages in both *S. spontaneum* and *S. officinarum*.

Heterologous expression of several STs in the defective yeast

To elucidate the potential functions of STs in *S. spontaneum* and *S. officinarum*, we expressed seven representative STs in the hexose transport-deficient *Saccharomyces cerevisiae* mutant strain EBY.VW4000, which is unable to grow on hexose or sucrose but does grow on the disaccharide maltose since 20 endogenous *ST* genes have been knocked out. The full-length cDNAs of *STP13*, *pGlcT2*, *TMT4*, *VGT3*, and *SUT1_T1* of *S. spontaneum* and *S. officinarum* were cloned separately into the pDRf1-GW vector (Figure 5b). The positive controls, *ScHXT5* of *S. cerevisiae* and *AtSUC2* of *A. thaliana*, were cloned separately into the pDRf1-GW vector.

After transformation into the yeast mutant strain EBY.VW4000, the growth ability of the yeast was investigated on selection culture medium containing 2% maltose, 2% glucose, 2% fructose, and 2% sucrose, with 2% maltose acting as the positive control (Figure 5c). The results showed that the exogenous expression of *STP13*, *pGlcT2*, and *VGT3* enabled the yeast to grow well on glucose and fructose medium, but not on sucrose medium. *SUT1_T1* exhibited the opposite results, indicating *STP13*, *pGlcT2*, or *VGT3* is sensitive to glucose and fructose, whereas *SUT1_T1* is sensitive to sucrose (Figure 5c). In addition, yeast transformed with *TMT4* grew well on the plates with glucose or fructose, and grew weakly on the plates with sucrose, indicating *TMT4* is sensitive to multiple kinds of sugar.

Divergence of *ST* co-expression network in *S. officinarum* and *S. spontaneum*

Weighted gene co-expression network analysis (WGCNA) (Langfelder and Horvath, 2008) was employed to construct gene networks using the RNA-seq data of 45 samples, including three different sugar accumulation stages, the developmental gradient leaf segments, and day-night rhythms, in these two *Saccharum* species, in which each node represents a gene and the connecting lines (edges) between genes represent the co-expression. The divergent *STs* expressed in these two *Saccharum* species were saved as the hub genes in order to explore the different co-expression networks in these two species. Of the 16 *STs* (marked in red color in Figure 6), five *STs* (*SUT1*, *SUT1_T1*, *STP4*, *STP7*, and *PLT17*) exhibited distinct co-expression in these two *Saccharum* species, with two *STs* (*SUT1* and *SUT1_T1*) being involved in a more complex co-expression network in *S. spontaneum* than in *S. officinarum* (Figure 6 and Figure S5). For example, 40 and 21 genes, including 'FAD dependent oxidoreductase' and 'H(+)-ATPase 2', were involved in the *SUT1* and *SUT1_T1* co-expression network in *S. officinarum*, while 153 and 170 genes, including 'Zinc finger superfamily', 'NBS-LRR', and 'fn3', showed co-expression with *SUT1* and *SU1_T1* in *S. spontaneum*. The remaining three *STs* (*STP4*, *STP7*, and *PLT17*) were included in more complex co-expression networks of *S. officinarum* than *S. spontaneum*.

DISCUSSION

Sugarcane is an important model crop for investigating sugar accumulation and carbohydrate metabolism. STs are considered as a crucial factor for carbohydrate allocation in the majority of higher plants, and STs have been characterized and analyzed in both prokaryotes and eukaryotes (Kruckeberg, 1996; Johnson and Thomas, 2007). However, the genome-wide identification and comprehensive analysis of this gene family in *S. spontaneum* has not been reported. The recently published *S. spontaneum* genome provided us with the opportunity to characterize the ST gene family and explore the mechanism of sugar accumulation in *S. spontaneum* (Zhang *et al.*, 2018).

© 2020 Society for Experimental Biology and John Wiley & Sons Ltd,

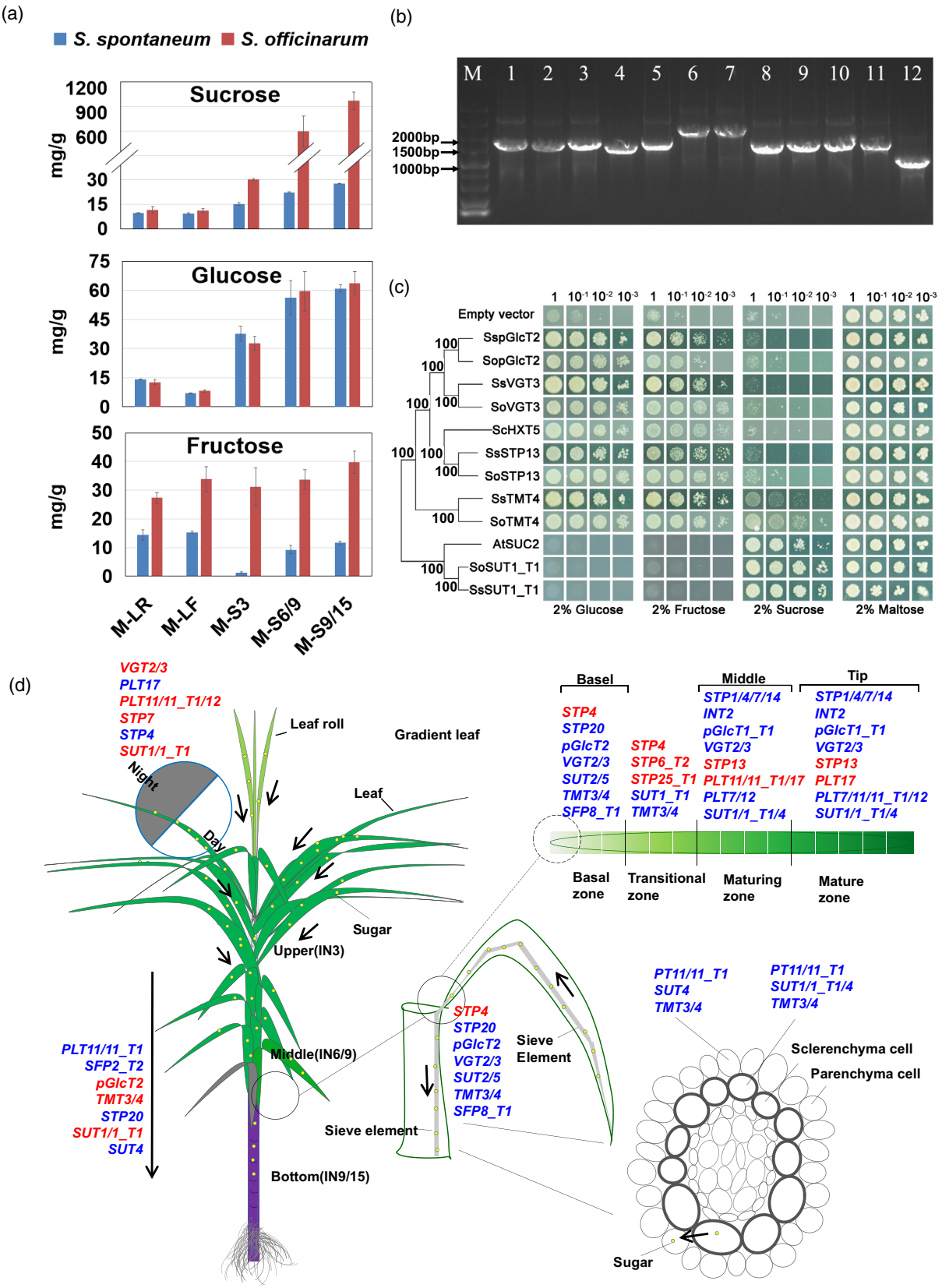

© 2020 Society for Experimental Biology and John Wiley & Sons Ltd,

Figure 5. The potential functions of STs in *S. spontaneum* and *S. officinarum*. (a) The characteristics of sugar metabolism in the matured leaf and matured stem of *S. spontaneum* and *S. officinarum*. The sugar concentration variation is presented in the histogram. (b) The cDNA clones of selected STs in *S. spontaneum* and *S. officinarum*. M: marker; 1: coding sequence (CDS) of *HXT5* in yeast; 2: CDS of *SsSTP13*; 3: CDS of *SoSTP13*; 4: CDS of *SspGlcT2*; 5: CDS of *SopGlcT2*; 6: CDS of *SsTMT4*; 7: CDS of *SoTMT4*; 8: CDS of *SsVGT3*; 9: CDS of *SoVGT3*; 10: CDS of *AtSUC2*; 11: CDS of *SoSUT1_T1*; 12: CDS of *SsSUT1_T1*. (c) Complementary effects of the hexose transport-defective yeast strain EBY.VW4000 by the heterologous expression of representative STs. The defective yeast strain EBY.VW4000 was transformed with empty pDRf1-GW, pDRf1-GW-ScHXT5, pDRf1-GW-Ss/SoSTP13, pDRf1-GW-Ss/SopGlcT2, pDRf1-GW-Ss/SoTMT4, pDRf1-GW-Ss/SoVGT3, pDRf1-GW-Ss/SoSUT1_T1, or pDRf1-GW-AtSUC2. The figure shows their growth on SD media containing different sugars as sole carbon source at 30°C for 3 days. EBY.VW4000 only grew well on SD media containing maltose, but not on the media containing other hexoses or sucrose. ScHXT5/AtSUC2 and the empty vector-transformed yeasts were used as the positive and negative controls, respectively. In each picture, the yeast strain was diluted to an OD_{600} value of 0.2 and then 1×, 10×, 100×, and 1000× diluted with sterile water. (d) Schematic models for expression patterns and physiological functions of the ST family during phloem loading and unloading based on gene expression profiles and sugar metabolic profiles in sugarcane. The STs marked with red color were differentially expressed between *S. spontaneum* and *S. officinarum*.

This study therefore initially analyzed the gene structure, motifs, and phylogenetics of the ST family in *S. spontaneum*, and identified a total of 105 STs in the *S. spontaneum* genome, which is more than in other species (62 in *S. bicolor*, 50 in *O. sativa*, 57 in *A. thaliana*, and 56 in *V. vinifera*). In *S. spontaneum* the ST genes were clustered into eight subfamilies, i.e., one sucrose transporter family and seven monosaccharide transporter families, based on the criteria defined in *A. thaliana* (Buttner, 2007), *V. vinifera* (Afoufa-Bastien *et al.*, 2010), and *O. sativa* (Johnson and Thomas, 2007). This might be caused by polyploidy of *S. spontaneum* with two additional WGDs taking place due to numerous tandem duplications (Zhang *et al.*, 2018). Interestingly, of the eight subfamilies, the PLT and STP subfamilies had the most members, similar to other monocots, which may be due to the repeated regions encompassed by STP and PLT genes (Li *et al.*, 2015). Furthermore, we have identified conserved domains in these eight subfamilies, and different motif compositions were identified in each of them, which were similar to those in *Pyrus* (Li *et al.*, 2015), *A. thaliana* (Buttner, 2007), and *V. vinifera* (Afoufa-Bastien *et al.*, 2010). The genes in the PLT, TMT, INT, and STP families were more conserved, with the number of exons ranging from one to six; in contrast, genes in the remaining four families (pGlcT, SUT, SFP, and VGT) had more exons. The same trend was found in ST families in *S. lycopersicum* (Reuscher *et al.*, 2014), indicating our classification of STs in *S. spontaneum* was accurate and reliable. In addition, the present study also found nine members in the SUT family, whereas a previous report identified six members (Zhang *et al.*, 2016). This difference in the number of family members may be caused by the incomplete coverage of BAC resources used in the earlier research. Therefore, the data from the intact *S. spontaneum* genome were provided to supplement the previous results.

Furthermore, we analyzed the gene expansion of the ST family in *S. spontaneum*. Gene duplication is well known to be a major driving force in gene expansion and neofunctionalization (Cannon *et al.*, 2004). Five mechanisms of gene duplications were proposed, including WGD (or polyploidization), tandem duplication, segmental duplication, transposon-mediated duplication, and retroduplication (Panchy *et al.*, 2016). Among those, tandem duplication, WGD, and segmental duplications occur most frequently in plants because most plants retain numerous duplicated chromosomal blocks within their genomes through polyploidy following chromosome rearrangements (Cannon *et al.*, 2004). Notably, a recent study revealed that both tandem duplication and WGD/segmental duplication contributed to the gene expansion of the *S. spontaneum* ST family (Zhang *et al.*, 2018), and although *S. spontaneum* experienced two independent rounds of WGD, tandem duplication was still the main mechanism for ST family expansion, with 62 ST genes undergoing tandem duplication. The same result was also found in *A. thaliana* and *O. sativa* (Johnson *et al.*, 2006; Buttner, 2007), but not in *Pyrus* (Li *et al.*, 2015). These results suggested tandem duplication played a major role in the expansion of the *ST* gene family in *S. spontaneum*. Furthermore, PLT and STP subfamilies were the major families that expanded significantly in *S. spontaneum*, which was similar to *O. sativa* (Johnson and Thomas, 2007) and *S. bicolor*, but not to other dicots, such as *A. thaliana* (Buttner, 2007) and *V. vinifera* (Afoufa-Bastien *et al.*, 2010), demonstrating the PLT and STP subfamilies may be related to monocot but not dicot evolution. In addition, the STP and PLT subfamilies were reported to have significant variations in size between the vascular and non-vascular lineages, suggesting the gene expansion of these two subfamilies could be related to the evolution of vascular plants (Johnson *et al.*, 2006).

Interestingly, recent research reported *S. spontaneum* was divided from the common ancestor of *S. spontaneum* and *S. bicolor* 7.779 million years ago (MYA) (Zhang *et al.*, 2019), and it then experienced two rounds of WGD accompanied by chromosome rearrangement events (Zhang *et al.*, 2018). In this study, the Ks value (mean Ks = 0.056) of tandem duplicated ST gene pairs showed that most ST tandem duplication events happened 4.307 MYA, which occurred after the divergence from *S. bicolor*. Similarly, the block comparative synteny of PLT and STP subfamilies between *S. spontaneum* and *S. bicolor* also support this point. In addition, the asymmetrical size of the block between *S. spontaneum* and *S. bicolor* might be caused by plentiful intergenic insertions in the *S. spontaneum*

© 2020 Society for Experimental Biology and John Wiley & Sons Ltd,

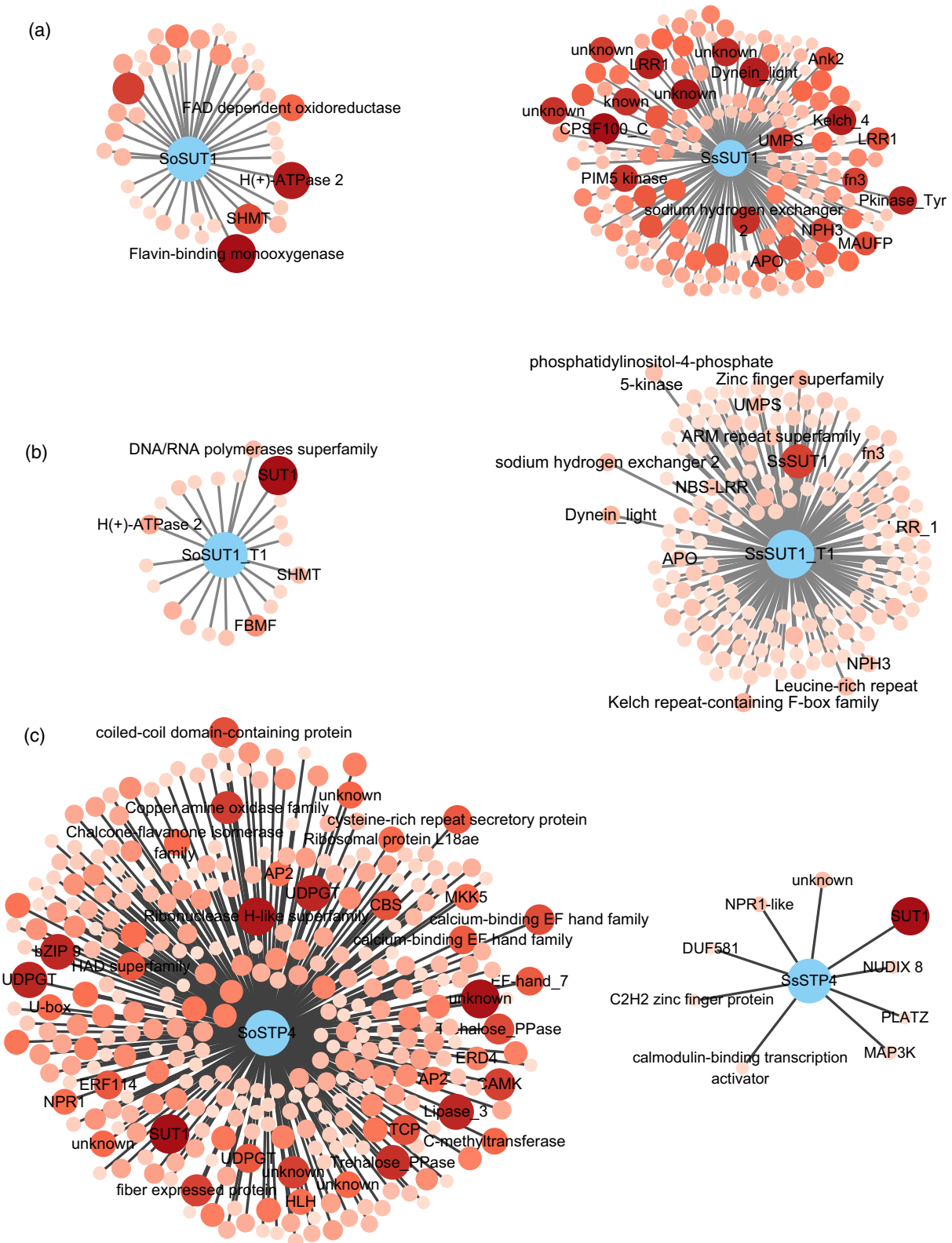

Figure 6. The correlation network of differentially expressed STs in *S. spontaneum* and *S. officinarum*. The correlation networks of *SUT1* (a), *SUT1_T1* (b), and *STP4* (c) in *S. officinarum* (left) and *S. spontaneum* (right), with each node representing a gene and the connecting lines (edges) between genes representing co-expression correlations. The circle size and color represent the weight value.

© 2020 Society for Experimental Biology and John Wiley & Sons Ltd,

genome, which provided the possibility for *ST* gene family evolution to take place (Sacher *et al.*, 1963).

The present study also investigated gene function divergence of *STs* in *Saccharum* through examining the expression of *ST* genes in the source and sink tissues, which provide an indication of the functional roles of the genes. Previous studies on STs demonstrated that they may play multiple roles during the different developmental stages in some plants (Afoufa-Bastien *et al.*, 2010; Wei *et al.*, 2014; Reuscher *et al.*, 2014; Li *et al.*, 2015). Therefore, we used four sets of RNA-seq data in two *Saccharum* species with different sugar contents for examining ST gene expression in order to determine the potential function of STs in *Saccharum*. In sugarcane, sucrose is initially hydrolyzed into fructose and glucose, and then re-synthesized during the transfer from the metabolic compartment to the storage compartment (Sacher *et al.*, 1963). All sugars diffuse slowly from the storage compartment, with reducing sugars diffusing more rapidly than sucrose (Glasziou, 1960). Immature storage tissues contain an invertase which is optimally active between pH 5.0 and pH 5.5 (Glasziou, 1962; Hatch *et al.*, 1963). This enzyme is absent in matured tissues, which contain higher levels of total sugars but little reducing sugar (Sacher *et al.*, 1963), indicating this enzyme could be responsible for the inversion of sucrose in the storage compartment (Hatch *et al.*, 1963).

The SUT subfamily was previously characterized based on BACs in *Saccharum*, and *SUT1* was predicted to play an enhanced role in directing the production of sucrose, leading to the accumulation in the source tissues of *Saccharum* species (Zhang *et al.*, 2016). In the present study, *SUT1* was highly expressed in the leaves, relatively matured stems, the mature zone of the leaf, and sclerenchyma cells, but undetectable in parenchymal cells. In contrast, *SUT1_T1* was highly expressed in those tissues, which was not discovered in the previous study carried out in the absence of the sugarcane genome, suggesting *SUT1* and *SUT1_T1* may play an important role in directing the production of sucrose in source tissues. Moreover, *SUT1_T1* enabled the yeast mutant EBY.VW4000 to grow well only on medium containing sucrose, indicating its substrate specificity for sucrose. Finally, the analysis of the co-expression network based on WGCNA showed that the expression of *SUT1* and *SUT1_T1* involved in the network was different between *S. spontaneum* and *S. officinarum*, suggesting they are affected differently in these two species, which may result in the differing abilities to transport sucrose.

In *S. spontaneum*, the expression of SUT1 and SUT1_T1 increased from 18:00 to 02:00, while in *S. officinarum* their expression increased from 06:00 to 10:00. The SUT proteins mainly have affinity for the disaccharide sucrose in *Saccharum* (Figure 5c), with sucrose being used for long-distance translocation in higher plants. In sugarcane, sucrose can be broken down rapidly for respiration and then re-synthesized in sinks, leading to a dynamic balance between storage and respiration or other metabolic uses (Wendler *et al.*, 1991). Therefore, we assumed that SUT1 and SUT1_T1 cooperated to provide the sugar for respiration in low-sucrose content *S. spontaneum* and to transport the sugar from source to sink for sugar accumulation during photosynthesis in the high-sucrose content *S. offincarum*. The majority of sucrose transporters have been characterized as H^+/sugar importers and are located at the plasma membrane, but in maize (*Zea mays*), a species close to sugarcane, a SUC4-type transporter was revealed to be a tonoplast-localized protein which releases sucrose from vacuoles (Carpaneto *et al.*, 2010; Schneider *et al.*, 2012). It is possible that these sucrose transporters retrieve sucrose from the vacuole in *S. spontaneum* during the night.

Most STPs or HTs identified in *A. thaliana* are located on the plasma membrane and have a broad substrate specificity, such as fructose, glucose, galactose, and mannose (Buttner, 2010). The results of the present study showed that *STP4* expression in the leaf and leaf roll of pre-mature and matured *S. spontaneum* was higher than in *S. officinarum*, which was the dominant gene expressed in those tissues of pre-mature and matured *S. spontaneum*, indicating *STP4* may play a role in sugar loading. *STP4* has a peak expression level in the leaf tissue during the daytime in both *Saccharum* species, and was also found to be mainly expressed in the developmental gradient leaf sections, especially in highly photosynthetic zones, of *S. spontaneum* and *S. officinarum*. The orthologs of *STP4* in *A. thaliana* and *V. vinifera* were proposed to transport hexose, and the orthologs in *O. sativa* are believed to participate in the transport of fructose/glucose from the apoplast to the cytosol (Cakir *et al.*, 2019). STP4 presented much higher expression levels in leaf and leaf rolls of pre-mature stages in *S. spontaneum* than in *S. officinarum*, supporting the fact that *S. spontaneum* mainly generates the monosaccharide, while *S. officinarum* accumulated sucrose. In addition, the co-expression network of *STP4* was divergent between *S. spontaneum* and *S. officinarum*, with 316 genes, including *bZIP9*, *ERF14*, and *AP2*, being involved in the co-expression network of *S. officinarum*, while only nine genes were included in *S. spontaneum*, indicating that the divergence of *STP4* expression in these two *Saccharum* species could be due to different regulatory networks. *STP7* and *STP13* were highly expressed in the leaves of seedling, pre-mature, and matured *S. spontaneum* as well as in *S. officinarum*, indicating that they are only expressed in leaves in a tissue-specific manner. In many leaved plants, the chloroplasts in the leaf tip are over-matured and display caducity, and most organs in these regions will be degraded to sugar or other small molecules for recycling. *STP13* was located in the plasma

© 2020 Society for Experimental Biology and John Wiley & Sons Ltd,

membrane, and was more highly expressed in the leaf tip zone of development gradient leaf sections in *S. officinarum* than in *S. spontaneum*. Further investigation found that *STP13* enabled the yeast mutant EBY.VW4000 to grow well with glucose and fructose, suggesting *STP13* has a function in retrieving the monosaccharides from senescent tissues. A previous study reported *STP13* was expressed in the leaf epidermal and mesophyll cells after flg22 treatment, and also considered STP13-mediated hexose uptake as a basal pathogen resistance mechanism (Dodds and Lagudah, 2016). Furthermore, *STP13* was expressed mainly in *S. officinarum* at night, indicating that its expression could be influenced by respiration, whereas *STP7* expression had a diurnal peak in the morning in both *S. officinarum* and *S. spontaneum*, suggesting *STP7* might be a sugar starvation-induced gene, since the depletion of nocturnal reserves also leads to the activation of sugar transport in both *S. officinarum* and *S. spontaneum*. *STP7* showed different co-expression networks between *S. spontaneum* and *S. officinarum*, indicating it may be associated with different mechanisms in these two species.

In *Saccharum*, *PLT11* and *PLT11_T1* were highly expressed in the matured leaf and stem of *S. officinarum* compared to *S. spontaneum*. *PLT11* and *PLT11_T1* were also mainly expressed in the photosynthetic regions of leaves, especially in daytime, which suggests they may play different roles in source and sink tissues. In many plants, sugar accumulation is source-limited in meristematic sinks and sink-limited in storage sinks (Smith and Stitt, 2007). *PLT11* and *PLT11_T1* were also expressed at high levels in sclerenchyma and parenchyma cells from the matured stalk (TPM > 800), implying *PLT11* and *PLT11_T1* may contribute to breaking the limitation of the storage sink, and thus give rise to the high sugar content in *S. officinarum*. In contrast, *PLT17* was mainly expressed in the leaf and the matured zone of the leaf in *S. officinarum*, and displayed peak levels in the morning, while it was undetectable in both sclerenchyma and parenchymal cells of the matured stalk in *S. officinarum*. Therefore, *PLT17* appears to be a sugar alcohol starvation-induced gene involved in sugar alcohol transport in the highly photosynthetic zones of *Saccharum*. Several roles have been suggested for sugar alcohols, including osmo-protection, quenching of reactive oxygen species, facilitation of boron transport, storage of reducing power, tolerance to salinity or drought, and involvement in plant–pathogen interactions (Loescher and Everard, 2000; Williamson *et al.*, 2002; Pommerrenig *et al.*, 2007), and they may serve as biomarkers and bioindicators for 21st-century plant breeding (Merchant and Richter, 2011).

The TMT subfamily has been characterized in *O. sativa* and *A. thaliana*, with proteins such as AtTMT1 and AtTMT2 being identified as fructose/H^+ or glucose antiporters that are localized to the vacuolar membrane (Wormit *et al.*, 2006; Schulz *et al.*, 2011), while BvTST2.1, the ortholog of AtTMT2 in sugar beet (*Beta vulgaris*), was also identified as a sucrose-specific transporter, and imported sucrose into the vacuole (Jung *et al.*, 2015). In this study, *TMT3* and *TMT4*, the orthologous gene pairs of *AtTMT2* and *AtTMT2*, were mainly expressed in the stem and transition regions of the leaf in both *Saccharum* species, and exhibited peak expression levels at nightfall, suggesting *TMT3* and *TMT4* may play a role in unloading in the sink. Surprisingly, *TMT4* not only enabled the yeast mutant EBY.VW4000 to survive on medium with glucose or fructose, but also on medium with sucrose, suggesting TMTs have a broad substrate specificity, which could enable different sugars to be used for sugar metabolism. In addition, *TMT3* and *TMT4* were also more highly expressed in parenchymal cells than in sclerenchyma cells, suggesting they may contribute to breaking the limits of the sink. *TMT4* was highly expressed in *S. spontaneum* during the daytime, while *TMT4* was highly expressed in *S. officinarum* during the nighttime. We expect that *TMT4* contributes to glucose accumulation in the low-sugar content *S. spontaneum*, which accumulated a much higher relative level of glucose during the day, while playing a key role in the transport of glucose resulting from the breakdown of sucrose required for respiration in the high-sucrose content *S. officinarum* during the night.

Similarly, VGTs were suggested to be localized to the plasma membrane and to function as sugar/H^+ antiporters loading sugars into the vacuole (Wormit *et al.*, 2006; Aluri and Büttner, 2007; Cho *et al.*, 2010; Schulz *et al.*, 2011).Three members of the VGT subfamily, *VGT2*, *VGT3*, and *VGT3_T1*, were expressed during the seedling, pre-mature, and matured stages. Of these, *VGT3* was mainly expressed in the leaves of *S. officinarum* compared to *S. spontaneum*, which had a similar expression pattern to *S. lycopersicum* (Reuscher *et al.*, 2014). In contrast to *TMT4*, *VGT3* displayed an expression peak in the morning in *S. officinarum* and at night in *S. spontaneum*. In Arabidopsis, TMTs were revealed to be the major glucose transporters for the Arabidopsis mesophyll vacuole rather than VGTs (Wormit *et al.*, 2006). It is likely that VGT3 contributes to monosaccharide accumulation in *S. officinarum* rather than TMT4, whereas VGT3 may also play a role in respiration during the night in *S. spontaneum*, as TMT does in *S. spontaneum*. Thus, TMT4 and VGT3 may contribute to the divergence in sugar accumulation trends between the two *Saccharum* species. Compared with *VGT3*, the other two members, *VGT2* and *VGT3_T1*, showed lower expression levels in the tissues of different stages, indicating they may not be the key members responsible for the accumulation of monosaccharides in *Saccharum*.

In addition, pGlcTs were isolated in chloroplast fractions and were suggested to function in sugar efflux from plastids in Arabidopsis (Weber *et al.*, 2000; Ferro *et al.*, 2003). In our study, two members of the *pGlcT* subfamily, *pGlcT1_T1* and *pGlcT2*, were expressed during three

© 2020 Society for Experimental Biology and John Wiley & Sons Ltd,

stages. Among them, *pGlcT2* showed higher expression in the tested internodes during the pre-matured and matured stages of *S. spontaneum* compared to *S. officinarum*, but not in the leaf development section and circadian rhythms of two species. This phenomenon could be explained by the fact that *S. spontaneum* mainly accumulated the monosaccharide, while *S. officinarum* mainly generated sucrose for storage. In contrast, *pGlcT1_T1* was expressed at a background level in all tissues, suggesting *pGlcT2* is a sink-specific gene, which may be responsible for sugar unloading in the sink tissues.

The sugars produced by photosynthesis are transported from the source leaf to the parenchyma cells of the sugarcane sink stalks through the sieve elements. Based on the sugar metabolic features, the expression patterns of 105 STs, and the heterologous expression of defective yeasts, we have proposed a model that summarizes the spatial and temporal expression of these genes in the cells and tissues of sugarcane plants (Figure 5d). In the photosynthetic leaf tissues, especially in the maturing and matured zones, *STP1/4/7/13/14*, *pGlcT1_T1*, *VGT2/3*, *INT2*, *PLT7/11/11_T1/12/17*, and *SUT1/1_T1/4* may play a primary role in exporting photosynthesized sugar or sugar alcohol from the leaf source tissue to the sink tissues, and *STP1/13* and *PLT12* may be responsible for retrieving the sugar in matured zones. Furthermore, the expression patterns of *VGT2/3*, *PLT11/11_T1/12/17*, *STP4/7*, and *SUT1/1_T1* were coordinated with the circadian rhythm, implying they may be influenced by sunlight and responsible for respiratory action. In the transition zone of the leaves, where photosynthesis is less active than in the maturing and matured zones, *STP4/6_T2/25_T1*, *SUT1_T1*, and *TMT3/4* may play a role in transporting sugars produced by photosynthesis. The basal zone serves as an immediate sink and connects the photosynthetic leaf tissue with the sink stalk, demonstrating *SUT2/5*, *STP4/20*, *SFP8_T1*, *pGlcT2*, *VGT2/3*, and *TMT3/4* may play primary roles in accommodating the products of photosynthesis and unloading these products from the leaves to stems. *PLT11/11_T1*, *SFP2_T2*, *pGlcT2*, *TMT3/4*, *STP20*, and *SUT1/1_T1/4* were expressed in the whole stalk during each developmental stage of *Saccharum*, indicating that they participate in the entire sugar accumulation process, while *PLT4* and *STP4* were primarily expressed in the pre-mature and matured stems, suggesting they may mediate the sugar efflux from the sieve elements in specific tissues. In addition, *PLT11/11_T1*, *SUT4*, and *TMT3/4* may also participate in sugar accumulation in parenchyma cells and sugar transport in sclerenchyma cells, with *SUT1/1_T1* possibly also being involved in sugar transport in sclerenchyma cells.

Conclusion

In the present study, we detected and analyzed 105 putative *ST* genes in the *S. spontaneum* genome, which were clustered into eight subfamilies. The PLT and STP subfamilies possessed more members than other subfamilies. Gene expansions were identified in the *S. spontaneum ST* family, which are likely caused by tandem duplications that occurred after *S. spontaneum* divergence from the common ancestor of *Saccharum* and *S. bicolor*. Expression analysis revealed *STP4* plays a role in the production of loading sugar, *STP13* has a function in retrieving sugar from senescent tissues, *STP7* is a sugar starvation-induced gene, *PLT11*, *PLT11_T1*, *TMT3*, and *TMT4* contribute to breaking the limitations of the storage sink, *PLT17* appears to be a sugar alcohol starvation-induced gene involved in sugar alcohol transport in *Saccharum*, and *SUT1* and *SUT1_T1* cooperate to provide the sugar for respiration. *VGT3* has different functions in these two *Saccharum* species. *pGlcT2* is a sink-specific gene that may be responsible for sugar unloading in the sink tissues. Despite an abundance of expression data for *Saccharum* STs to predict their functions, the cooperation of the network of *ST* genes is still unknown. Our current data provide an important basis and direction for future research aiming to understand the functions of the *ST* genes and the molecular mechanisms of sucrose accumulation in *Saccharum*, and we also put forward a promising direction for molecular breeding in *Saccharum*.

EXPERIMENTAL PROCEDURES

Plant materials

Two *Saccharum* species with different sugar contents, LA-Purple (*S. officinarum*, $2n = 8x = 80$, high sugar content) and SES208 (*S. spontaneum*, $2n = 8x = 64$, low sugar content), were used in this study. Sugarcane seedlings were grown in soil-filled plastic pots under standard conditions (at a light intensity of 350 μmol m^{-2} sec^{-1}, 14 h/10 h light (L)/dark (D), 30°C L/22°C D, and 60% relative humidity) in a greenhouse and then transferred to clay loam soil after 5–6 weeks. Stem and leaf tissues from seedlings were collected at 35 days from both *Saccharum* species. Leaf rolls, leaves, and internodes were harvested from well-watered 10- to 12-month-old plants. The internode numbers on the sugarcane stalk were determined as described previously (Moore, 1987). Briefly, the internode number 1 was the node below the top visible dewlap (TVD) leaf sheath attachment, and additional internodes were numbered consecutively down the stalk (Moore, 1987). In sugarcane, the upper internodes contain lower levels of sucrose than the bottom internodes, and thus the upper internode was considered as the immature internode while the bottom internode was considered as the mature internode (Vorster and Botha, 1999; Uys *et al.*, 2007). We selected the upper (internode 3 in both *S. offincarum* and *S. spontaneum*), middle (internode 9 in *S. offincarum* and internode 6 in *S. spontaneum*), and bottom internodes (internode 15 in *S. offincarum* and internode 9 in *S. spontaneum*) from 12-month-old *S. offincarum* and *S. spontaneum* for this study. For clarification, we have drawn a schematic diagram to illustrate the sampling of these tissues (Figure S6). The tissues were wrapped in foil paper, frozen in liquid nitrogen, and then stored at −80°C before RNA extraction.

© 2020 Society for Experimental Biology and John Wiley & Sons Ltd,

Identification of ST protein in *S. spontaneum*

All *ST* genes in the *S. spontaneum* monoploid genome downloaded from Pfam (http://pfam.sanger.ac.uk/) were searched using HMMER software with E-value < 1E−5 based on the *Sugar_tr* domain (PF00083). The identified *ST* gene candidates were further confirmed based on the known *STs* from *A. thaliana* and *O. sativa* as a query through the Basic Local Alignment Search Tool (BLAST) (Altschul *et al.*, 1997). Finally, a total of 105 credible *STs* were identified from the *S. spontaneum* monoploid genome for further analysis.

Distribution and duplication of *ST* genes on pseudo-molecular chromosomes

Using the general feature format files (gff3) of *ST* genes from the *S. spontaneum* monoploid genome database, the distribution of *ST* genes in *S. spontaneum* monoploid pseudo-chromosomes was drawn using R. The duplication pattern for each *ST* gene was analyzed, and 35 519 protein-coding genes from the *S. spontaneum* monoploid genome database were analyzed by an all-vs-all local BLAST search with E-value < 1E−5. The BLAST result was imported into MCScanX software (http://chibba.pgml.uga.edu/mcscan2/) for identifying tandem duplications and WGD/segmental duplications with default parameters (Wang *et al.*, 2012).

Phylogenetic analysis of the *ST* gene family

Based on the alignment of protein sequences, the phylogenetic tree of the *ST* gene family was constructed by NJ methods. The construction of the NJ tree was carried out using MEGA (version 7.0) with the 'pairwise deletion' option and the 'Poisson correction' model (Kumar *et al.*, 2016), and the reliability of internal branches was valued by the bootstrapping of 1000 replicates. These results were then imported into the interactive tree of life (iTOL) program for creating the phylogenetic tree (Letunic and Bork, 2016).

Ka/Ks calculation of tandem duplications

The coding sequence of tandem duplications for *ST* gene pairs was selected to calculate non-synonymous (Ka) and synonymous (Ks) substitution ratios by the Nei–Gojobori method (Kumar *et al.*, 2016). If Ka/Ks > 1, this indicates that the gene pairs are under positive selection, while Ka/Ks < 1 indicates purifying selection and Ka/Ks = 1 indicates neutral evolution.

Gene structure, conserved motifs, and physicochemical properties of *STs*

The conserved motifs of *ST* genes in *S. spontaneum* were analyzed using the MEME suite 4.11.1 program (http://meme.nbcr.net/meme/cgi-bin/meme.cgi) with the following parameters: optimum width, 15–60; maximum number of motifs, 600; number of repetitions, any; and maximum number of motifs, 15. The results were then imported into the TBtools program (Chen *et al.*, 2020) to display the conserved motifs for each *ST* gene. GSDS (http://gsds.cbi.pku.edu.cn) was used to determine the structure of *ST* genes (Hu *et al.*, 2015), and ExPASy (http://web.expasy.org/compute_pi/) was used to predict the isoelectric point and relative molecular mass of ST proteins. The amino acid sequences of the deduced proteins were submitted to the TMHMM Server v.2.0 (http://www.cbs.dtu.dk/services/TMHMM/) for predicting transmembrane domains and to WoLF PSORT (http://wolfpsort.hgc.jp) for predicting the subcellular localization of ST proteins.

Yeast heterologous expression of STs

The DNA sequence open reading frames (ORFs) of *STP13*, *pGlcT2*, *TMT4*, *VGT3*, and *SUT1_T1* were amplified by PCR based on the cDNA from *S. spontaneum* and *S. officinarum*. The ORFs of *ScHXT5* and *AtSUC2* were cloned with primers containing the attB adapter from *S. cerevisiae* and *A. thaliana*, respectively, and then inserted into the yeast expression vector pDRf1-GW with Gateway™ cloning (Xuan *et al.*, 2013). The constructed vectors of Ss/SoSTP13-pDRf1-GW, Ss/SopGlcT2-pDRf1-GW, Ss/SoTMT4-pDRf1-GW, Ss/SoVGT3-pDRf1-GW, Ss/SoSUT1_T1-pDRf1-GW, ScHXT5-pDRf1-GW, and AtSUC2-pDRf1-GW were verified by Sanger sequencing, and then introduced into the yeast mutant EBY.VW4000, which is defective in hexose transport, using PEG/Li Ac-mediated transformation (Gietz and Schiestl, 2007). Yeast transformants were incubated on selective dropout (SD, -URA) medium containing 2% maltose as a carbon source for 2–3 days at 30°C. The presence of the constructed vectors in the yeast transformants was further verified by plasmid isolation and resequencing. For complementation growth assays, the transformants were grown in YNB liquid medium containing 2% maltose overnight, washed twice in sterile water, and then resuspended at an OD_{600} value of 0.2. Subsequently, serial dilutions (×1, ×10, ×100, ×1000) were plated on SD (-URA) media containing either 2% maltose as positive control or 2% glucose, 2% fructose, or 2% sucrose. Growth was recorded after 2–4 days at 30°C.

Analysis of soluble sugar content

Tissue samples were obtained from 12-month-old sugarcane for the leaf roll, leaf, top immature internode (Stem 3), pre-matured internode (Stem 6 for *S. spontaneum* and Stem 9 for *S. officinarum*), and matured internode (Stem 9 for *S. spontaneum* and Stem 15 for *S. officinarum*) as previously described (Chen *et al.*, 2017). Approximately 0.1–0.2-g samples were used to determine the soluble sugar (TSS) content, and each sample was assayed with three replicates. Sugar was extracted using the soluble sugar (Sucrose, Fructose, D-Glucose) determination kit (Meike Biotechnology Co., Ltd, China). TSS concentrations were determined using a Thermo Fisher spectrophotometer (Type: 1510) according to the manufacturer's protocol. The detailed protocol for the kit is as follows.

Collect tissue in a 50-ml microcentrifuge tube and freeze by dipping in liquid nitrogen. Grind the tissue using a mortar and pestle. Transfer up to 0.1 g frozen ground plant tissue to a new 2-ml microcentrifuge tube for sucrose, fructose, and D-glucose determination.

D-Glucose determination. Add 1 ml distilled water and vortex at maximum speed to mix thoroughly. Place in a 100°C water bath for 10 min. Cool and centrifuge at 8000 ***g*** for 10 min at room temperature. For the test tube (*A*1), transfer 100 μl lysate to a new 2-ml microcentrifuge tube and add 900 μl mixed solution including glucose oxidase, peroxidase, 4-aminoantipyrine, and phenol. For the control tube (*A*2), mix 100 μl distilled water and 900 μl mixed solution. For the standard tube (*A*3), mix 100 μl glucose standard solution (0.5 μmol ml^{-1}) and 900 μl mixed solution. Measure the OD_{505} value with a spectrophotometer. Glucose content was calculated as follows:

$$\text{Glucose content}\,(\mu\text{mol ml}^{-1}) = \frac{0.5\,\mu\text{mol ml}^{-1} \times 100\,\mu\text{l} \times (A1 - A2) \div (A3 - A2)}{0.1\,\text{g} \div (100\,\mu\text{l} + 900\,\mu\text{l}) \times 100\,\mu\text{l}}$$

Fructose determination. Add 1 ml extract solution and vortex 1 min. Place in an 80°C water bath for 10 min and oscillate three

© 2020 Society for Experimental Biology and John Wiley & Sons Ltd,

to five times. Cool and centrifuge at 4000 ***g*** for 10 min at room temperature. Transfer the lysate to a new 2-ml microcentrifuge tube, add 2 mg activated carbon, and allow decolorization at 80°C for 30 min. Add 1 ml extract solution and centrifuge at 4000 ***g*** for 10 min at room temperature. For the test tube (*A1*), transfer 100 μl lysate to a new 2-ml microcentrifuge tube and add 900 μl mixed solution including phosphoric acid and resorcinol. For the control tube (*A2*), mix 100 μl distilled water and 900 μl mixed solution. For the standard tube (*A3*), mix 100 μl fructose standard solution (5 mg ml^{-1}) and 900 μl mixed solution. Mix well at 80°C for 10 min. Cool and measure the OD_{480} value with a spectrophotometer. Fructose content was calculated as follows:

$$\text{Fructose content}\left(\text{mg g}^{-1}\right)=\frac{5\,\text{mg ml}^{-1}\times 100\,\mu\text{l}\times(A1-A2)\div(A3-A2)}{0.1\,\text{g}}$$

Sucrose determination. Add 1 ml extract solution and vortex 1 min. Place in an 80°C water bath for 10 min and oscillate three to five times. Cool and centrifuge at 4000 ***g*** for 10 min at room temperature. Transfer the lysate to a new 2-ml microcentrifuge tube, add 2 mg activated carbon, and allow decolorization at 80°C for 30 min. Add 1 ml extract solution and centrifuge at 4000 ***g*** for 10 min at 25°C. For the test tube (*A*1), transfer 100 μl lysate to a new 2-ml microcentrifuge tube and add 50 μl NaOH solution. For the control tube (*A*2), mix 100 μl distilled water and 50 μl NaOH solution. For the standard tube (*A*3), mix 100 μl fructose standard solution (1 mg ml^{-1}) and NaOH solution. Mix well and place at 100°C for 5 min. Add 900 μl mixed solution including phosphoric acid and resorcinol to *A*1, *A*2, and *A*3. Mix well and place at 100°C for 10 min. Cool and measure the OD_{480} value with a spectrophotometer. Sucrose content was calculated as follows:

$$\text{Sucrose content}\left(\text{mg g}^{-1}\right)=\frac{1\,\text{mg ml}^{-1}\times 100\,\mu\text{l}\times(A1-A2)\div(A3-A2)}{0.1\,\text{g}\times 100\,\mu\text{l}\div 2\,\text{ml}}$$

Gene expression analysis by RNA-seq

RNA-seq data were obtained from the same sources as in our previous work (Zhang *et al.*, 2016), including the following sugarcane tissues: seedling stem and leaves, the top internode (i.e., internode 3), a maturing internode (i.e., internode 9 for 'LA-Purple' and 6 for 'SES208' due to the long internode), and a matured internode (i.e., internodes 15 and 9 for 'LA-Purple' and 'SES208', respectively) from 10- to 12-month-old plants. The *Saccharum* RNA-seq database was aligned to the reference gene models of *S. spontaneum* genome by Trinity with default settings (Grabherr *et al.*, 2013). RNA-seq quantitative analysis was completed by Trinity transcript quantification and the TPM value was calculated by the RNA-seq by expectation–maximization method.

Validation of ST expression by qRT-PCR

RNA (≤1 μg) from each tissue was reverse-transcribed to cDNA using a Reverse Transcriptase Kit (Takara, Beijing, China) in a 20-μl reaction volume with 1 μl of random primers and 1 μl of mixed poly-dT primers (18–23 nt). Gene-specific primers (Table S1) were designed using the online Primer Quest tool (http://www.idtdna.com/Primerquest/Home/Index) from Integrated DNA Technologies. qRT-PCR was performed by a Multicolor Real-Time PCR Detection System (Bio-Rad, Hercules, CA, USA). The PCR conditions were: 95°C for 30 sec, followed by 40 cycles at 95°C for 5 sec, 60°C for 30 sec, and 95°C for 10 sec. Melting curve analysis was performed to confirm PCR specificity with a heat dissociation protocol from 65°C to 95°C following the final cycle of PCR. To normalize the expression data, the glyceraldehyde-3-phosphate dehydrogenase (*GAPDH*) and eukaryotic elongation factor 1a (*eEF-1a*) genes (Ling *et al.*, 2014) were used as internal controls, and three replicates were performed for each sample. The relative expression levels for each *ST* gene in different tissues of the two *Saccharum* species were calculated with the $2^{-\Delta\Delta Ct}$ method (Livak and Schmittgen, 2001).

Co-expression network construction of STs

The whole genes of the *S. spontaneum* genome were clustered into the gene co-expression network by the R package 'WGCNA' (Langfelder and Horvath, 2008). The genes with TPM < 0.001 were filtered and the parameters for this network were set as follows: power = 12, MEDissThres = 0.25, nSelect = 400. Finally, the *ST* genes were chosen as hub genes to construct the co-expression network, and the candidate genes were imported into the network generation tool Cytoscape v3.7.1 (Shannon *et al.*, 2003) (https://cytoscape.org/) to visualize the interactors.

ACKNOWLEDGMENTS

This work was supported by the Science and Technology Planting Project of Guangdong Province (2019B020238001); the National Key Research and Development Program (2018YFD1000104); the National High-tech R&D Program (2013AA100604); the National Natural Science Foundation of China (31201260, 31760413, and 31660420); the Science and Technology Major Project of Guangxi (AA17202025); the Fujian Provincial Department of Education (No. JA12082); the China Scholarship Council (201707877011); and the Scientific Research Foundation of the Graduate School of Fujian Agriculture and Forestry University (324-1122yb050).

AUTHOR CONTRIBUTIONS

JZ designed the experiments. QZ, XH, HL, JZ, and YY conceived the study. QZ, XH, HL, JZ, YS, MZ, RM, ZW, and YY performed the experiments and analyzed the data. QZ and JZ wrote the manuscript. All the authors read and approved the final article.

CONFLICT OF INTEREST

The authors have no conflict of interest to declare.

DATA AVAILABILITY STATEMENT

Saccharum spontaneum gene sequence data and the related RNA-seq data of this study can be found in the Sugarcane database (SGD, http://sugarcane.zhangjiselab.cn/sgd/html/index.html). The gene sequences of other species used in the study can be obtained from Phytozome (https://phytozome.jgi.doe.gov/pz/portal.html).

SUPPORTING INFORMATION

Additional Supporting Information may be found in the online version of this article.

Figure S1. Phylogenetic tree of the SFP subfamily from representative monocotyledons and dicotyledons.

Figure S2. Phylogenetic tree of the SUT subfamily from representative monocotyledons and dicotyledons.

Figure S3. Phylogenetic relationships, gene structures, and conserved protein motifs of the *S. spontaneum* ST superfamily. (a)

© 2020 Society for Experimental Biology and John Wiley & Sons Ltd,

The neighbor-joining (NJ) tree on the left includes 105 ST genes from *S. spontaneum*. The ST genes were clustered into nine subfamilies. (b) Exon/intron structures of ST genes from *S. spontaneum*. Exons and introns are represented by black boxes and black lines, respectively. (c) Architecture of conserved protein motifs in nine subfamilies. Each motif is represented by a colored box.

Figure S4. qRT-PCR verification of four STs transcriptome expression profile. Comparison of RNA-seq data (blue bar) with qRT-PCR data (red line). The normalized expression level (TPM) of RNA-seq data is indicated on the left *y*-axis. The relative qRT-PCR expression level is shown on the right y-axis. Actin was used as the internal control. Both methods showed similar gene expression trends (color figure online).

Figure S5. The correlation network of differentially expressed STs in two *Saccharum* species. The correlation networks of STP7 (a) and PLT17 (b) in *S. officinarum* (left) and *S. spontaneum* (right), with each node representing a gene and the connecting lines (edges) between genes representing co-expression correlations. The circle size and color indicate the degree of gene interaction.

Figure S6. Schematic diagram illustrating the tissue collections of internodes in *S. spontaneum* and *S. officinarum*. The upper (internode 3 in both *S. offincarum* and *S. spontaneum*), middle (internode 9 in *S. offincarum* and internode 6 in *S. spontaneum*), and bottom internodes (internode 15 in *S. offincarum* and internode 9 in *S. spontaneum*) from 12-month-old *S. offincarum* and *S. spontaneum* were collected for this study.

Table S1. The primers used for qRT-PCR in *Saccharum*.

Table S2. Comparison of SUT subfamily genes in *S. spontaneum* and *S. bicolor*.

Table S3. The Ka/Ks ratios of tandem duplication gene pairs.

REFERENCES

Afoufa-Bastien, D., Medici, A., Jeauffre, J., Coutos-Thevenot, P., Lemoine, R., Atanassova, R. and Laloi, M. (2010) The Vitis vinifera sugar transporter gene family: phylogenetic overview and macroarray expression profiling. *BMC Plant Biol.* **10**, 245.

Altschul, S.F., Madden, T.L., Schaffer, A.A., Zhang, J., Zhang, Z., Miller, W. and Lipman, D.J. (1997) Gapped BLAST and PSI-BLAST: a new generation of protein database search programs. *Nucleic Acids Res.* **25**, 3389–3402.

Aluri, S. and Büttner, M. (2007) Identification and functional expression of the Arabidopsis thaliana vacuolar glucose transporter 1 and its role in seed germination and flowering. *Proc. Natl Acad. Sci. USA*, **104**, 2537–2542.

Aoki, N., Hirose, T., Scofield, G.N., Whitfeld, P.R. and Furbank, R.T. (2003) The sucrose transporter gene family in rice. *Plant Cell Physiol.* **44**, 223–232.

Boorer, K.J., Loo, D.D. and Wright, E.M. (1994) Steady-state and presteady-state kinetics of the H+/hexose cotransporter (STP1) from *Arabidopsis thaliana* expressed in Xenopus oocytes. *J. Biol. Chem.* **269**, 20417–20424.

Bull, T. and Glasziou, K. (1963) The Evolutionary significance of sugar accumulation in Saccharum. *Aust. J. Biol. Sci.* **16**, 737–742.

Buttner, M. (2007) The monosaccharide transporter(-like) gene family in Arabidopsis. *FEBS Lett.* **581**, 2318–2324.

Buttner, M. (2010) The Arabidopsis sugar transporter (AtSTP) family: an update. *Plant Biol.* **12**(Suppl 1), 35–41.

Cakir, B., Tian, L., Crofts, N. *et al.* (2019) Re-programming of gene expression in the CS8 rice line over-expressing ADPglucose pyrophosphorylase induces a suppressor of starch biosynthesis. *Plant J.* **97**, 1073–1088.

Cannon, S.B., Mitra, A., Baumgarten, A., Young, N.D. and May, G. (2004) The roles of segmental and tandem gene duplication in the evolution of large gene families in Arabidopsis thaliana. *BMC Plant Biol.* **4**, 10.

Carpaneto, A., Geiger, D., Bamberg, E., Sauer, N., Fromm, J. and Hedrich, R. (2005) Phloem-localized, proton-coupled sucrose carrier ZmSUT1 mediates sucrose efflux under the control of the sucrose gradient and the proton motive force. *J. Biol. Chem.* **280**, 21437–21443.

Carpaneto, A., Koepsell, H., Bamberg, E., Hedrich, R. and Geiger, D. (2010) Sucrose- and H-dependent charge movements associated with the gating of sucrose transporter ZmSUT1. *PLoS One*, **5**, e12605.

Casu, R.E., Grof, C.P., Rae, A.L., McIntyre, C.L., Dimmock, C.M. and Manners, J.M. (2003) Identification of a novel sugar transporter homologue strongly expressed in maturing stem vascular tissues of sugarcane by expressed sequence tag and microarray analysis. *Plant Mol Biol.* **52**, 371–386.

Chang, A.B., Lin, R., Studley, W.K., Tran, C.V. and Saier, M.H. (2004) Phylogeny as a guide to structure and function of membrane transport proteins (Review). *Mol. Membr. Biol.* **21**, 171–181.

Chen, C., Chen, H., Zhang, Y. *et al.* (2020) TBtools: An integrative toolkit developed for interactive analyses of big biological data. *Mol. Plant.* **13**, 1194–1202.

Chen, L.Q., Hou, B.H., Lalonde, S. *et al.* (2010) Sugar transporters for intercellular exchange and nutrition of pathogens. *Nature*, **468**, 527–532.

Chen, L.Q., Qu, X.Q., Hou, B.H., Sosso, D., Osorio, S., Fernie, A.R. and Frommer, W.B. (2012) Sucrose efflux mediated by SWEET proteins as a key step for phloem transport. *Science*, **335**, 207–211.

Chen, Y., Zhang, Q., Hu, W. *et al.* (2017) Evolution and expression of the fructokinase gene family in Saccharum. *BMC Genom.* **18**, 197.

Cho, J.I., Burla, B., Lee, D.W. *et al.* (2010) Expression analysis and functional characterization of the monosaccharide transporters, OsTMTs, involving vacuolar sugar transport in rice (*Oryza sativa*). *New Phytol.* **186**, 657–668.

Deol, K.K., Mukherjee, S., Gao, F., Brule-Babel, A., Stasolla, C. and Ayele, B.T. (2013) Identification and characterization of the three homeologues of a new sucrose transporter in hexaploid wheat (*Triticum aestivum* L.). *BMC Plant Biol.* **13**, 181.

Dodds, P.N. and Lagudah, E.S. (2016) Starving the enemy. *Science*, **354**, 1377–1378.

ElSayed, A.I., Ramadan, M.F. and Komor, E. (2010) Expression of sucrose transporter (ShSUT1) in a Hawaiian sugarcane cultivar infected with Sugarcane yellow leaf virus (SCYLV). *Physiol. Mol. Plant. P*, **75**, 56–63.

Ferro, M., Salvi, D., Brugiere, S. *et al.* (2003) Proteomics of the chloroplast envelope membranes from Arabidopsis thaliana. *Mol. Cell Proteomics.* **2**, 325–345.

Gietz, R.D. and Schiestl, R.H. (2007) High-efficiency yeast transformation using the LiAc/SS carrier DNA/PEG method. *Nat Protoc.* **2**, 31.

Glasziou, K.T. (1962) Accumulation and transformation of sugars in sugar cane stalks: mechanism of inversion of sucrose in the inner space. *Nature*, **193**, 1100.

Glasziou, K.T. (1960) Accumulation and transformation of sugars in sugar cane stalks. *Plant Physiol.* **35**, 895–901.

Grabherr, M.G., Haas, B.J., Yassour, M., Levin, J.Z. and Amit, I. (2013) Trinity: reconstructing a full-length transcriptome without a genome from RNA-Seq data. *Nat. Biotechnol.* **29**, 644.

Hatch, M.D., Sacher, J.A. and Glasziou, K.T. (1963) Sugar accumulation cycle in sugar cane. I. Studies on enzymes of the cycle. *Plant Physiol.* **38**, 338–343.

Hu, B., Jin, J., Guo, A.Y., Zhang, H., Luo, J. and Gao, G. (2015) GSDS 2.0: an upgraded gene feature visualization server. *Bioinformatics*, **31**, 1296–1297.

Johnson, D.A., Hill, J.P. and Thomas, M.A. (2006) The monosaccharide transporter gene family in land plants is ancient and shows differential subfamily expression and expansion across lineages. *BMC Evol. Biol.* **21**, 6–64.

Johnson, D.A. and Thomas, M.A. (2007) The monosaccharide transporter gene family in Arabidopsis and rice: a history of duplications, adaptive evolution, and functional divergence. *Mol. Biol. Evol.* **24**, 2412–2423.

Juchaux-Cachau, M., Landouar-Arsivaud, L., Pichaut, J.P. *et al.* (2007) Characterization of AgMaT2, a plasma membrane mannitol transporter from celery, expressed in phloem cells, including phloem parenchyma cells. *Plant Physiol.* **145**, 62–74.

Julius, B.T., Leach, K.A., Tran, T.M., Mertz, R.A. and Braun, D.M. (2017) Sugar transporters in plants: new insights and discoveries. *Plant Cell Physiol.* **58**, 1442–1460.

Jung, B., Ludewig, F., Schulz, A. *et al.* (2015) Identification of the transporter responsible for sucrose accumulation in sugar beet taproots. *Nat. Plants*, **1**, 14001.

© 2020 Society for Experimental Biology and John Wiley & Sons Ltd,

Kühn, C. (2003) A comparison of the sucrose transporter systems of different plant species. *Plant Biol.* **5**, 215–232.

Kühn, C. and Grof, C.P. (2010) Sucrose transporters of higher plants. *Curr. Opin. Plant Biol.* **13**, 288–298.

Klemens, P.A., Patzke, K., Trentmann, O. *et al.* (2014) Overexpression of a proton-coupled vacuolar glucose exporter impairs freezing tolerance and seed germination. *New Phytol.* **202**, 188–197.

Kruckeberg, A.L. (1996) The hexose transporter family of *Saccharomyces cerevisiae*. *Arch Microbiol.* **166**, 283–292.

Kumar, S., Stecher, G. and Tamura, K. (2016) MEGA7: molecular evolutionary genetics analysis version 7.0 for bigger datasets. *Mol. Biol. Evol.* **33**, 1870–1874.

Langfelder, P. and Horvath, S. (2008) WGCNA: an R package for weighted correlation network analysis. *BMC Bioinformatics*, **9**, 559.

Lemoine, R. (2000) Sucrose transporters in plants: update on function and structure. *Biochim. Biophys. Acta*, **1465**, 246–262.

Letunic, I. and Bork, P. (2016) Interactive tree of life (iTOL) v3: an online tool for the display and annotation of phylogenetic and other trees. *Nucleic Acids Res.* **44**, W242–245.

Li, J.M., Zheng, D.M., Li, L.T., Qiao, X., Wei, S.W., Bai, B., Zhang, S.L. and Wu, J. (2015) Genome-wide function, evolutionary characterization and expression analysis of sugar transporter family genes in pear (*Pyrus bretschneideri* Rehd). *Plant Cell Physiol.* **56**, 1721–1737.

Ling, H., Wu, Q., Guo, J., Xu, L. and Que, Y. (2014) Comprehensive selection of reference genes for gene expression normalization in sugarcane by real time quantitative rt-PCR. *PLoS One*, **9**, e97469.

Livak, K.J. and Schmittgen, T.D. (2001) Analysis of relative gene expression data using real-time quantitative PCR and the 2(-Delta Delta C(T)) Method. *Methods*, **25**, 402–408.

Loescher, W.H. and Everard, J.D. (2000) *Regulation of Sugar Alcohol Biosynthesis*. Dordrecht: Springer.

Merchant, A. and Richter, A. (2011) Polyols as biomarkers and bioindicators for 21st century plant breeding. *Funct. Plant Biol.* **38**, 934–940.

Milne, R.J., Byrt, C.S., Patrick, J.W. and Grof, C.P. (2013) Are sucrose transporter expression profiles linked with patterns of biomass partitioning in Sorghum phenotypes? *Front. Plant Sci.* **4**, 223.

Moore, J.W., Herrera-Foessel, S., Lan, C. *et al.* (2015) A recently evolved hexose transporter variant confers resistance to multiple pathogens in wheat. *Nat. Genet.* **47**, 1494–1498.

Moore, P.H. (1987) Anatomy and morphology. *Dev. Crop Sci.* **11**, 85–142.

Noiraud, N., Maurousset, L. and Lemoine, R. (2001) Identification of a mannitol transporter, AgMaT1, in celery phloem. *Plant Cell*, **13**, 695–705.

Panchy, N., Lehti-Shiu, M. and Shiu, S.H. (2016) Evolution of gene duplication in plants. *Plant Physiol.* **171**, 2294–2316.

Pommerrenig, B., Papiniterzi, F.S. and Sauer, N. (2007) Differential regulation of sorbitol and sucrose loading into the phloem of plantago major in response to salt stress. *Plant Physiol.* **144**, 1029–1038.

Poschet, G., Hannich, B., Raab, S. *et al.* (2011) A novel Arabidopsis vacuolar glucose exporter is involved in cellular sugar homeostasis and affects the composition of seed storage compounds. *Plant Physiol.* **157**, 1664–1676.

Rae, A.L., Perroux, J.M. and Grof, C.P.L. (2005) Sucrose partitioning between vascular bundles and storage parenchyma in the sugarcane stem: a potential role for the ShSUT1 sucrose transporter. *Planta*, **220**, 817–825.

Reinders, A., Sivitz, A.B., Hsi, A., Grof, C.P., Perroux, J.M. and Ward, J.M. (2006) Sugarcane ShSUT1: analysis of sucrose transport activity and inhibition by sucralose. *Plant Cell Environ.* **29**, 1871–1880.

Reuscher, S., Akiyama, M., Yasuda, T., Makino, H., Aoki, K., Shibata, D. and Shiratake, K. (2014) The sugar transporter inventory of tomato: genome-wide identification and expression analysis. *Plant Cell Physiol.* **55**, 1123–1141.

Riesmeier, J.W., Willmitzer, L. and Frommer, W.B. (1992) Isolation and characterization of a sucrose carrier cDNA from spinach by functional expression in yeast. *EMBO J.* **11**, 4705–4713.

Sacher, J.A., Hatch, M.D. and Glasziou, K.T. (1963) Sugar accumulation cycle in sugar cane. III. Physical & metabolic aspects of cycle in immature storage tissues. *Plant Physiol.* **38**, 348–354.

Sauer, N. (2007) Molecular physiology of higher plant sucrose transporters. *FEBS Lett.* **581**, 2309–2317.

Sauer, N. and Tanner, W. (1989) The hexose carrier from Chlorella. cDNA cloning of a eucaryotic H+-cotransporter. *FEBS Lett.* **259**, 43–46.

Schneider, S., Hulpke, S., Schulz, A. *et al.* (2012) Vacuoles release sucrose via tonoplast-localised SUC4-type transporters. *Plant Biol.* **14**, 325–336.

Schulz, A., Beyhl, D., Marten, I. *et al.* (2011) Proton-driven sucrose symport and antiport are provided by the vacuolar transporters SUC4 and TMT1/2. *Plant J.* **68**, 129–136.

Shannon, P., Markiel, A., Ozier, O. *et al.* (2003) Cytoscape: a software environment for integrated models of biomolecular interaction networks. *Genome Res.* **13**, 2498–2504.

Smith, A.M. and Stitt, M. (2007) Coordination of carbon supply and plant growth. *Plant Cell Environ.* **30**, 1126–1149.

Sreenivasan, T.V. and Nair, N.V. (1991) *Catalogue on Sugarcane Genetic Resources. 111. Saccharum oflicinarum L.* Coimbatore: Sugarcane Breeding Institute.

Stadler, R., Buttner, M., Ache, P. *et al.* (2003) Diurnal and light-regulated expression of AtSTP1 in guard cells of Arabidopsis. *Plant Physiol.* **133**, 528–537.

Uys, L., Botha, F.C., Hofmeyr, J.H.S. and Rohwer, J.M. (2007) Kinetic model of sucrose accumulation in maturing sugarcane culm tissue. *Phytochemistry*, **68**, 2375–2392.

Vorster, D.J. and Botha, F.C. (1999) Sugarcane internodal invertases and tissue maturity. *J. Plant Physiol.* **155**(4–5), 470–476.

Truernit, E., Stadler, R., Baier, K. and Sauer, N. (1999) A male gametophyte-specific monosaccharide transporter in Arabidopsis. *Plant J.* **17**, 191–201.

Wang, Y., Tang, H., Debarry, J.D. *et al.* (2012) MCScanX: a toolkit for detection and evolutionary analysis of gene synteny and collinearity. *Nucleic Acids Res.* **40**, e49.

Weber, A., Servaites, J.C., Geiger, D.R., Kofler, H., Hille, D., Groner, F., Hebbeker, U. and Flugge, U.I. (2000) Identification, purification, and molecular cloning of a putative plastidic glucose translocator. *Plant Cell*, **12**, 787–802.

Wei, X., Liu, F., Chen, C., Ma, F. and Li, M. (2014) The *Malus domestica* sugar transporter gene family: identifications based on genome and expression profiling related to the accumulation of fruit sugars. *Front. Plant Sci.* **5**, 569.

Wendler, R., Veith, R., Dancer, J., Stitt, M. and Komor, E. (1991) Sucrose storage in cell suspension cultures of Saccharum sp. (sugarcane) is regulated by a cycle of synthesis and degradation. *Planta*, **183**, 31–39.

Williamson, J.D., Jennings, D.B., Guo, W.W., Pharr, D.M. and Ehrenshaft, M. (2002) Sugar Alcohols, Salt Stress, and Fungal Resistance: Polyols—Multifunctional Plant Protection? *J. Am. Soc. Hortic. Sci.* **127**(4), 467–473.

Wormit, A., Trentmann, O., Feifer, I. *et al.* (2006) Molecular identification and physiological characterization of a novel monosaccharide transporter from Arabidopsis involved in vacuolar sugar transport. *Plant Cell*, **18**, 3476–3490.

Xuan, Y.H., Hu, Y.B., Chen, L.Q., Sosso, D., Ducat, D.C., Hou, B.H. and Frommer, W.B. (2013) Functional role of oligomerization for bacterial and plant SWEET sugar transporter family. *Proc. Natl. Acad. Sci. USA*, **110**, E3685–3694.

Yamada, K., Saijo, Y., Nakagami, H. and Takano, Y. (2016) Regulation of sugar transporter activity for antibacterial defense in Arabidopsis. *Science*, **354**, 1427–1430.

Zhang, J., Zhang, Q., Li, L. *et al.* (2019) Recent polyploidization events in three Saccharum founding species. *Plant Biotechnol. J.* **17**, 264–274.

Zhang, J., Zhang, X., Tang, H. *et al.* (2018) Allele-defined genome of the autopolyploid sugarcane Saccharum spontaneum L. *Nat. Genet.* **50**, 1565–1573.

Zhang, J., Zhou, M., Walsh, J., Zhu, L., Chen, Y. and Ming, R. (2014) *Sugarcane Genetics and Genomics*. Hoboken: John Wiley & Sons Ltd.

Zhang, Q., Hu, W., Zhu, F., Wang, L., Yu, Q., Ming, R. and Zhang, J. (2016) Structure, phylogeny, allelic haplotypes and expression of sucrose transporter gene families in Saccharum. *BMC Genom.* **17**, 88.

© 2020 Society for Experimental Biology and John Wiley & Sons Ltd,

View publication stats